Research of Photocathode RFgun at SPring-8

Hirofumi HANAKI

JASRI/SPring-8

Contents

1. Introduction

- 1.1 Direction of the Research
- 1.2 History
- 1.3 Characteristics of SPring-8 RF gun

1.1 Direction of the Research

- Lowest Emittance Beam Generation based on
  - 3D Laser Shaping
  - 3D Beam Dynamics Simulation
  - Cavity Technology for Higher RF Field
  - New Cathode Developments
  - High Resolution Emittance Monitor

1.2 History

1996 Study of photocathode RFguns started for the next generation photon source

1999 First beam test
A new laser system ordered

2001 New Ti:Sapphire laser system installed

2002 Emittance 2 πmmmrad@0.1nC
Cartridge type cathode development started

2003 New gun test room constructed and an accelerating structure installed

2004 Maximum field of 190 MV/m at cathode

1.3 Characteristics of SPring-8 RFgun

1. Laser

- THG of Ti:Sa Laser (263 nm, 10Hz, 200 μJ/pulse)
- Spatial profile control : Pinhole & Homogenizer
- Temporal distribution : Stretched with SiO_2 glass rods
- Energy stability : 2% rms with homogenizer & pinhole

2. RF cavity

- S-band (2856MHz), Single-cell pill-box type
- Cathode : cavity wall or cathode plug in a vacuum cartridge
- High electric field on cathode : 190 MV/m

3. Synchronization of Laser & RF

- RF generation(2856 MHz) from laser pulses(89.25 MHz)
- RMS jitter (@low level) < 100 fs

2. Laser

- 2.1 Laser System Configuration
- 2.2 Laser & RF Synchronization
- 2.3 Laser Profile Control
- 2.4 Long-term Stability of Laser

2.1 Laser System Configuration

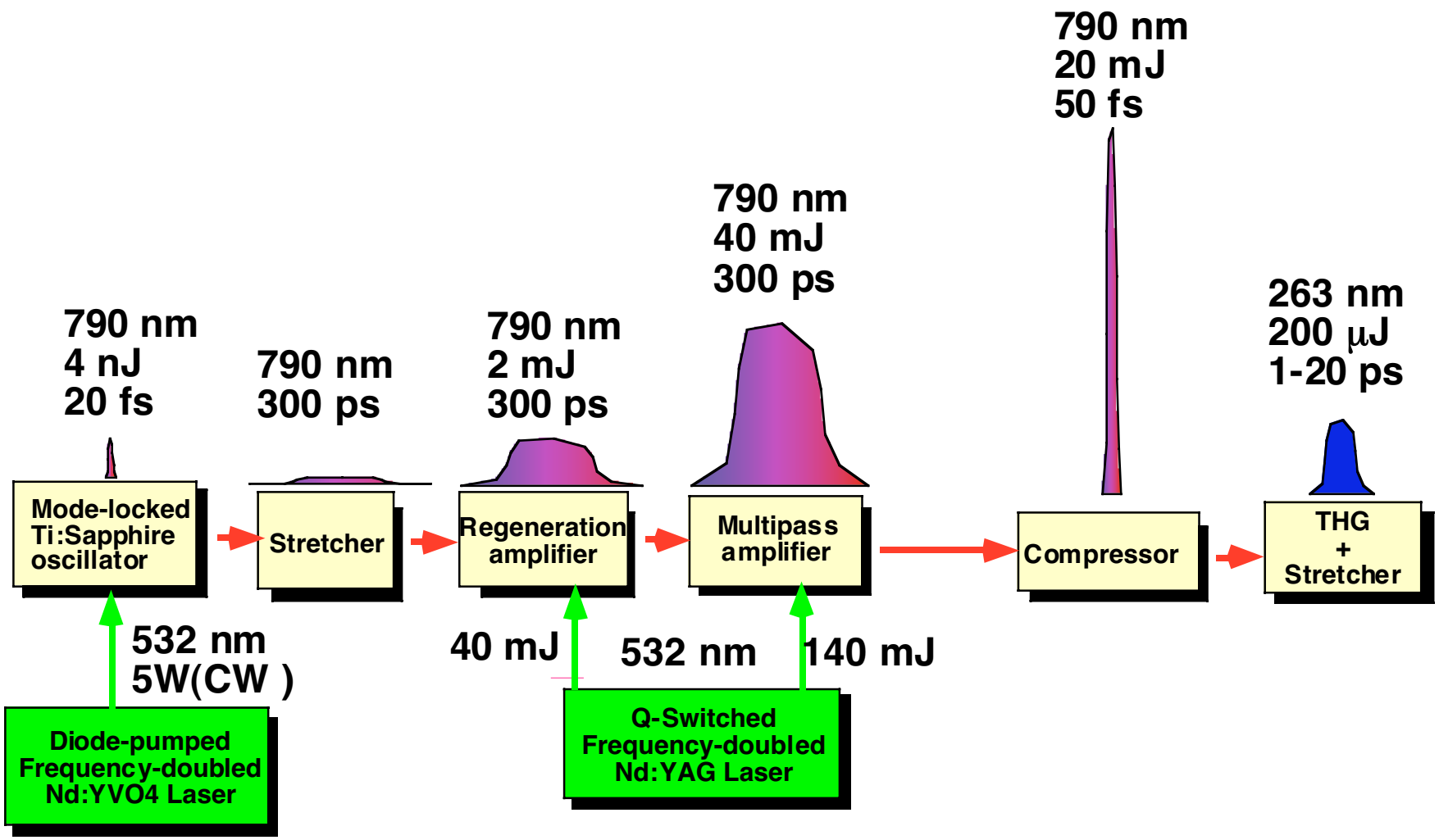

2.2 Laser & RF Synchronization

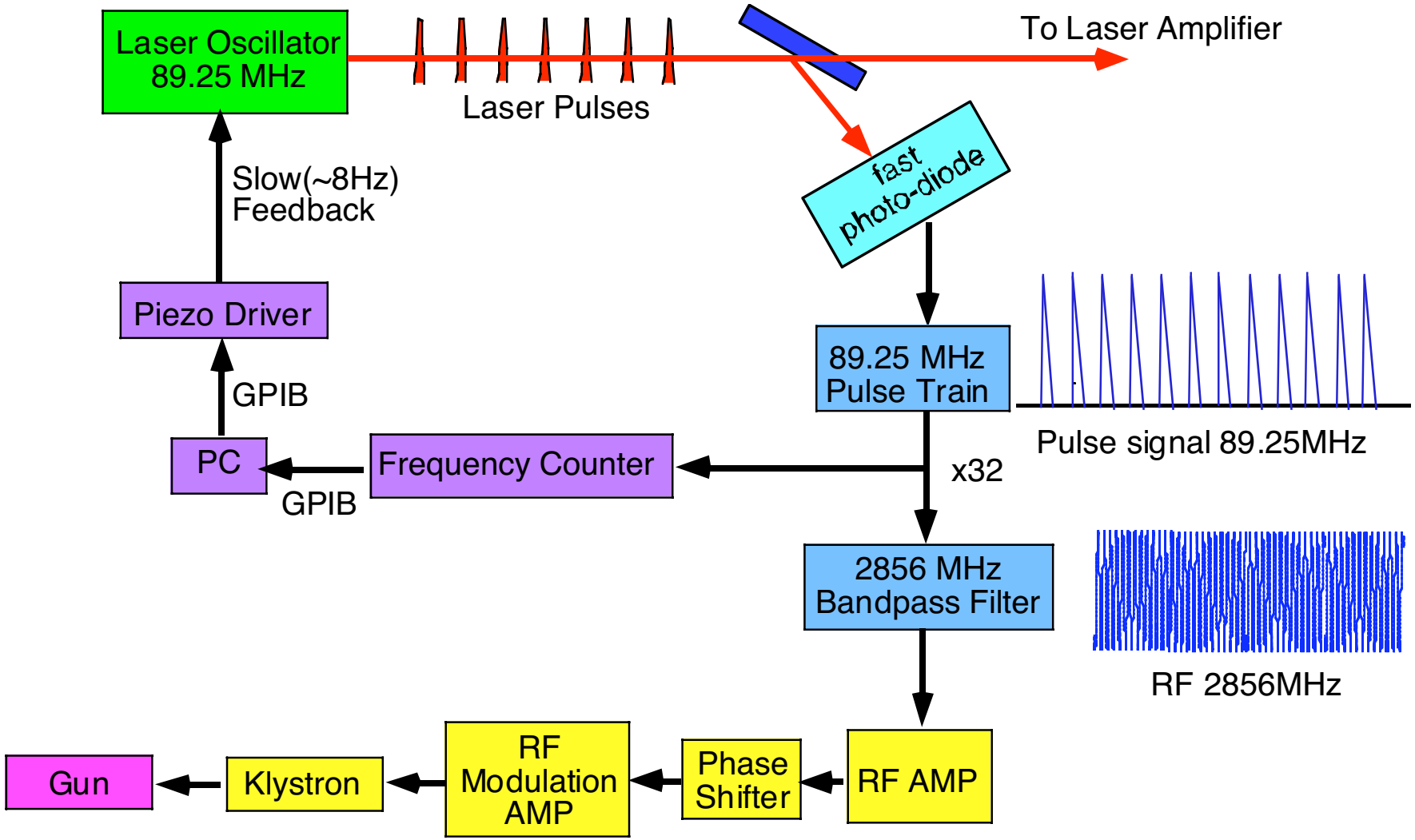

Short Time Jitter Measurement

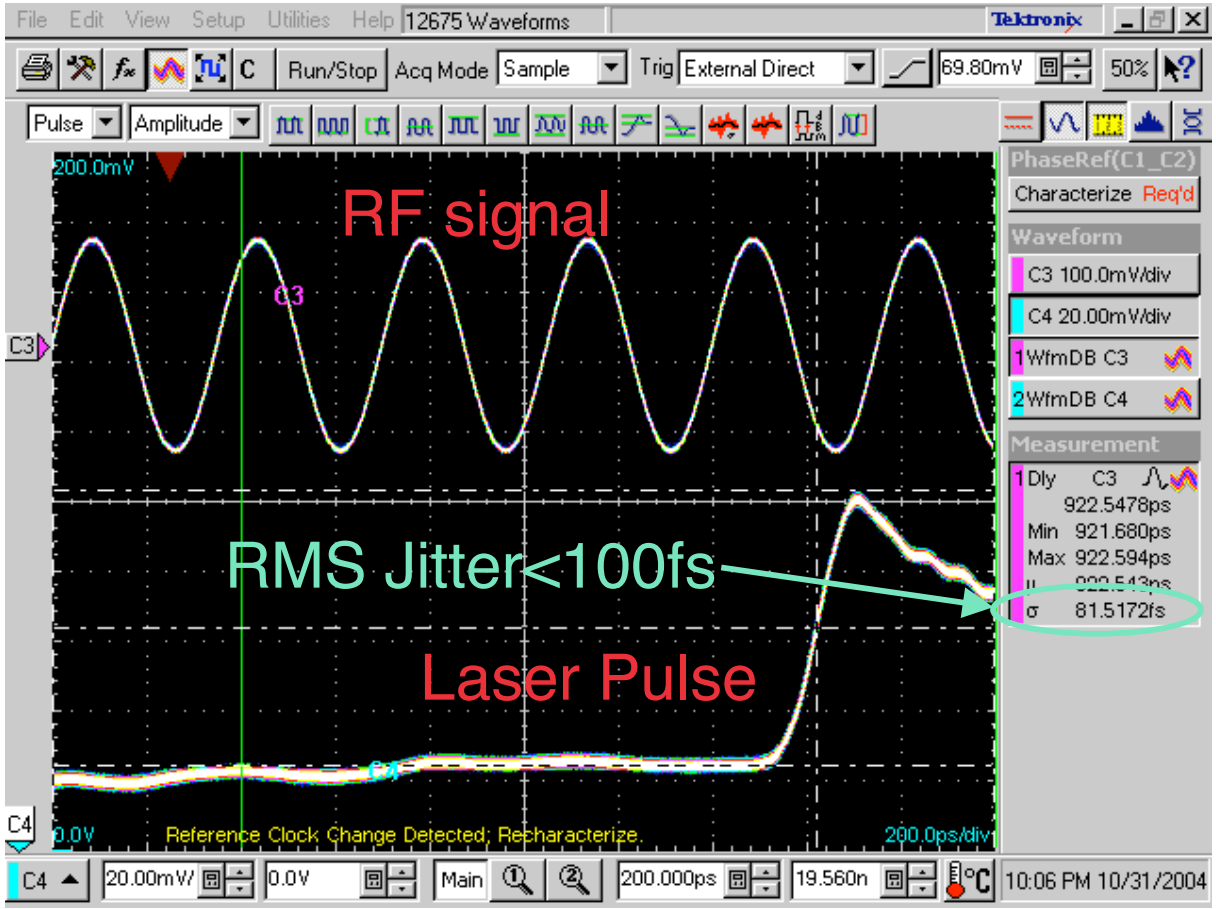

Time delay between RF signal & Laser pulse measured with Tektronix TDS8200 Sampling Oscilloscope

2-3. Optimization of laser profiles

~ Spatial & Temporal ~

Beam Quality Control by

Spatial Shaping

- **Microlens Array**
- **Deformable Mirror**

Pulse (Temporal) Shaping

- **SLM (Spatial Light Modulator)**

Wave Front Control

- **Deformable Mirror**

2.3.1 Physical background of ideal laser profile

$$\sigma = \sqrt{\sigma_{SC}^2 + \sigma_{RF}^2 + \sigma_{Th}^2}$$

Space charge effect consists of:

1. **Linear term in radial direction**
   - **possible to compensate with Solenoid Coils**
2. **Non-linear term in radial direction**
   - **possible to suppress non-linear effects with optimization of ideal Laser Profile**

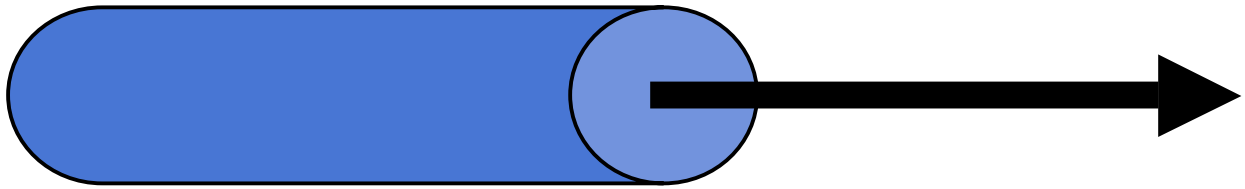

2.3.2 Spatial shaping with microlens array

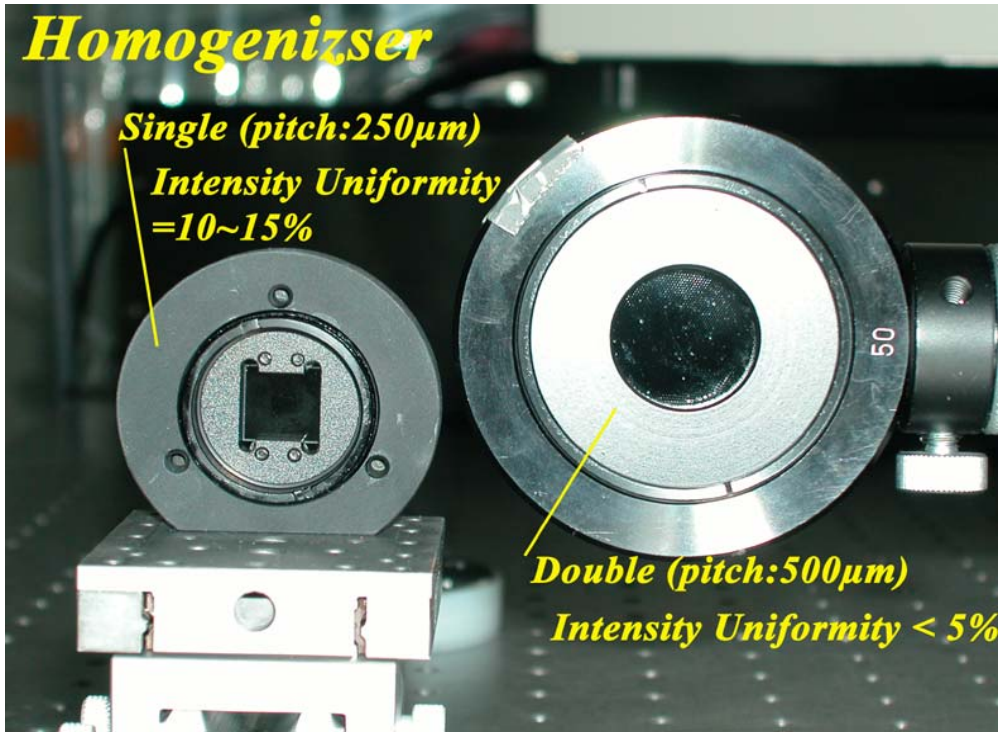

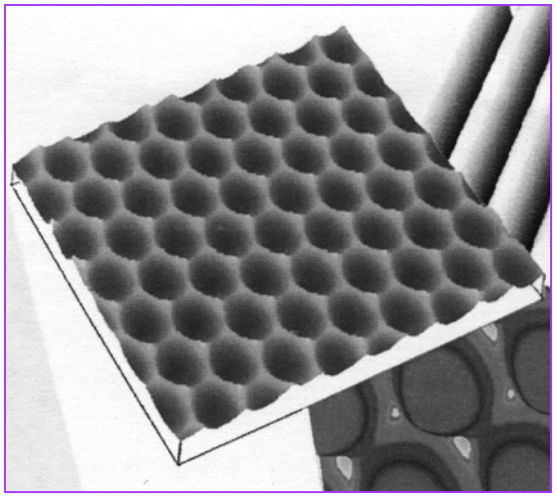

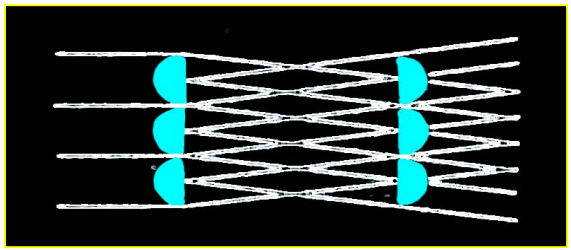

Structure of Microlens Array
and the function

2.3.3 Measurement of Laser Pulse Profile

Spatial:

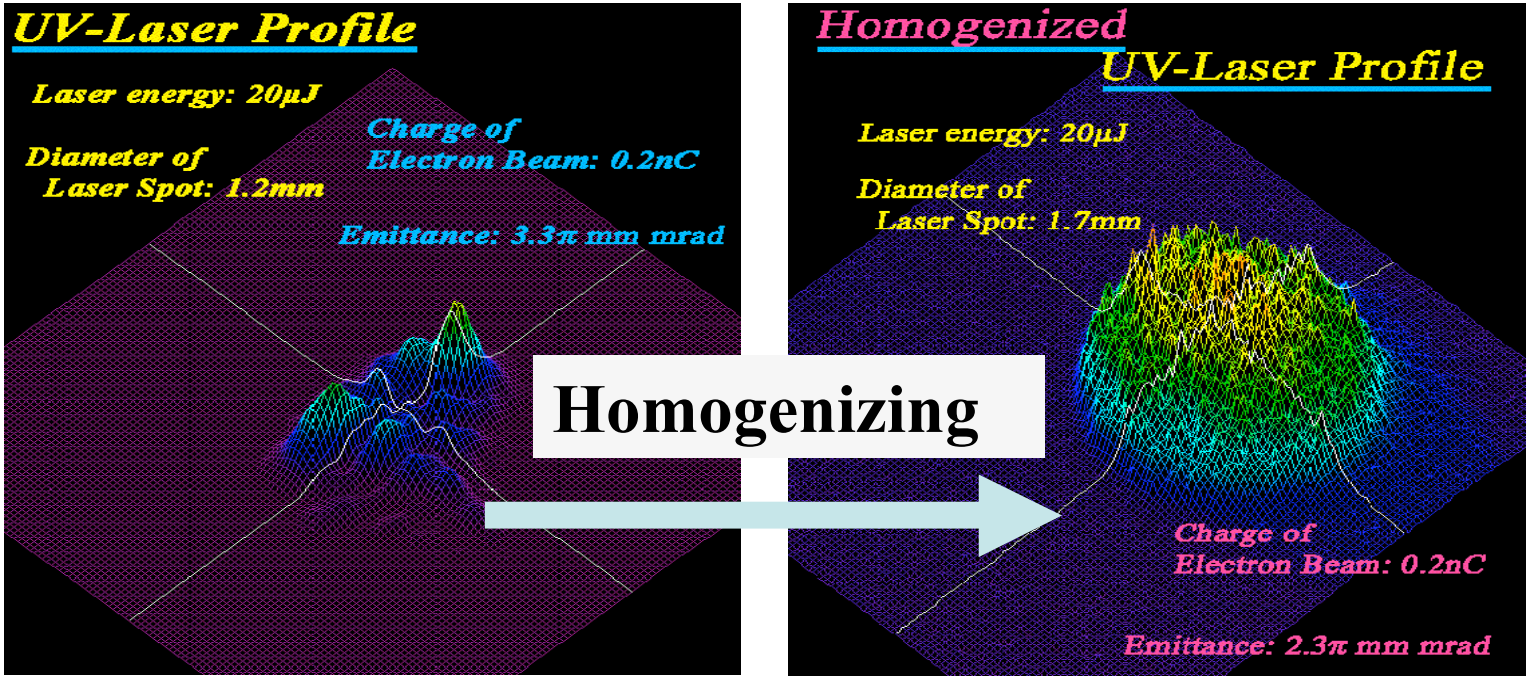

Temporal:

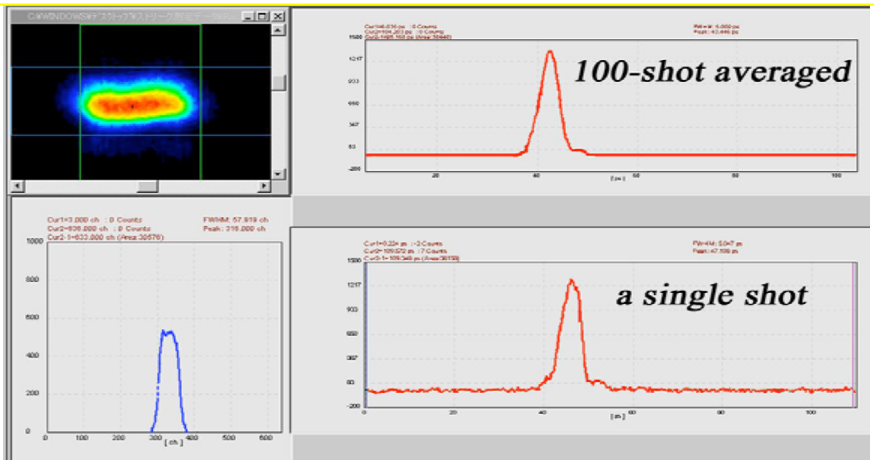

Spot size: 2.0 mm

Pulse width: 5 ps

(45-cm Fused Silica ×2)

2.3.4 Automatic laser-beam control system

- Computer-aided **SLM (Spatial Light Modulator)**
  ⇨ **Rectangular Pulse shaping**
- Computer-aided **DM (Deformable mirror)**
  ⇨ **Flattop spatial profile**

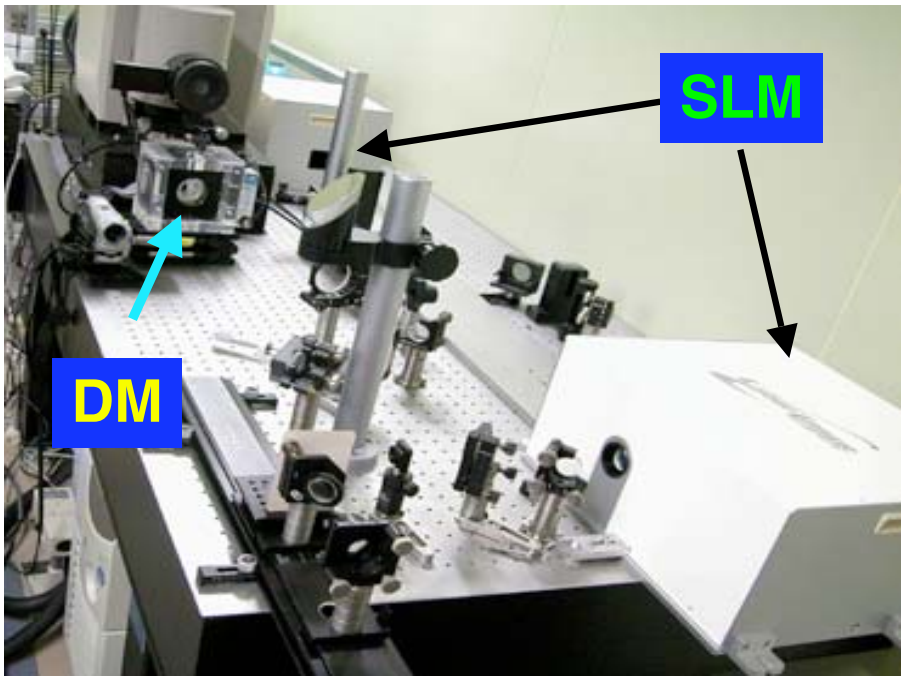

Automatic Control Optics
- **Spatial shaping (DM)**
- **Pulse shaping (SLM)**
- **Wave front Control (DM)**

2.3.5 Pulse shape control with SLM

Short laser pulse

Grating — breaks a light pulse into a spectrum
(Transform time distribution to spatial distribution)

SLM — modulates intensity of the spectrum

Grating — transforms the spectrum into a light pulse

Shaped laser pulse

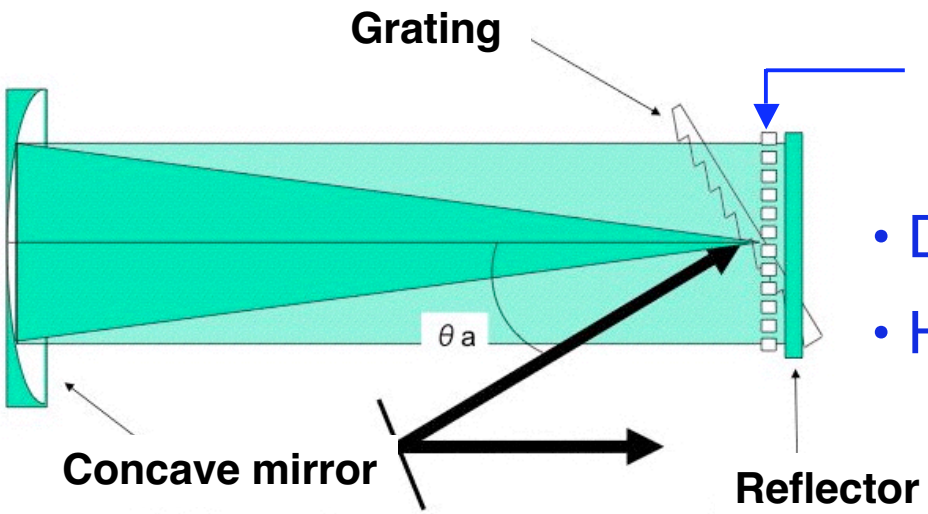

Utilizing silica plate modulator

- Directly shaping for UV-Laser
- Higher Laser power threshold

2.3.6 Spatial shaping with Deformable Mirror

Mirror cell: 59
Deformation step: 256

⇨ **Combination: 256^{59} !**

AI-Algorism for spatial shaping is under development

DM
Double reflection

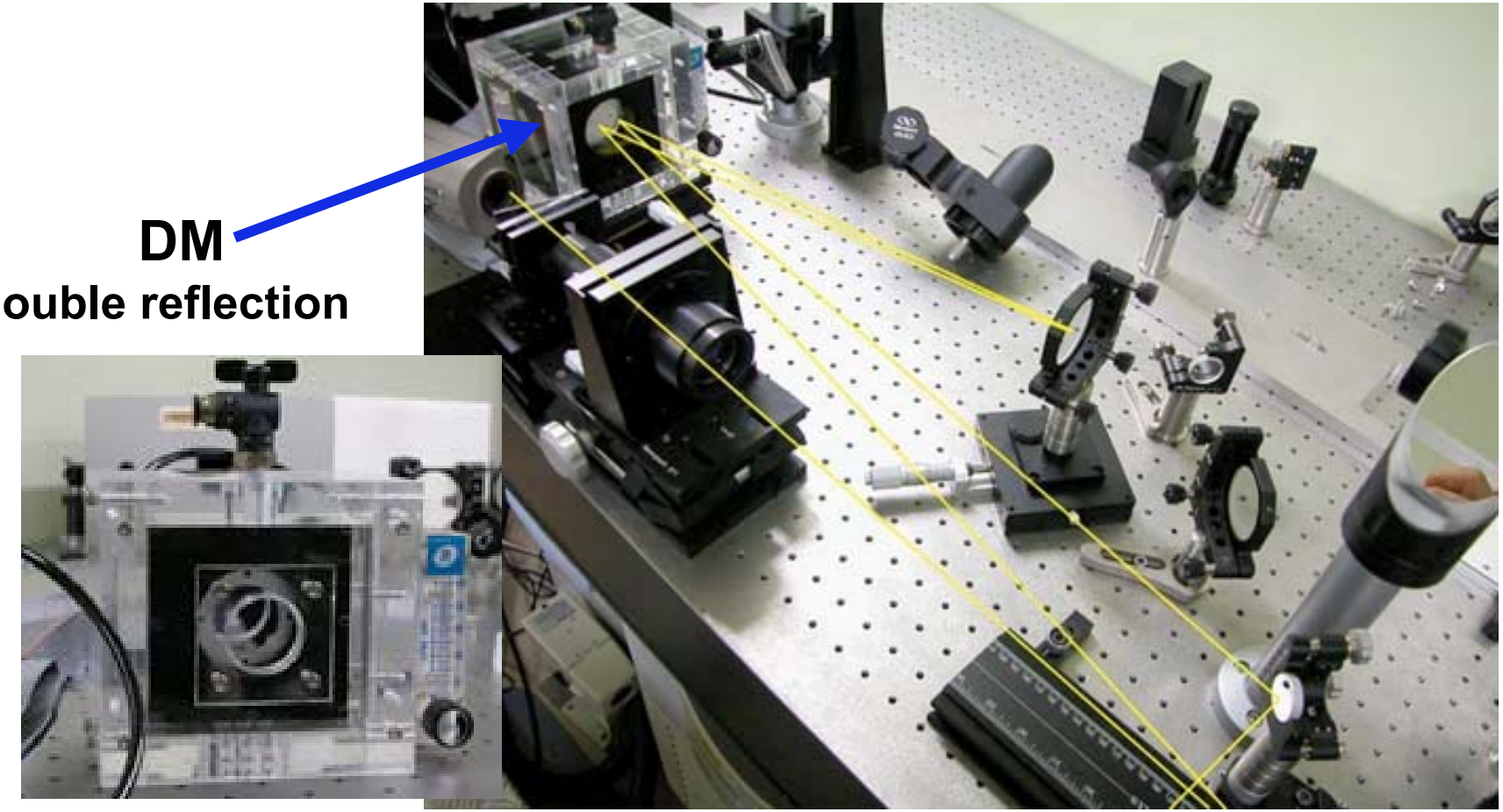

Structure of DM-Actuator:

Voltage: 0 ~ 255 V

Actuator:

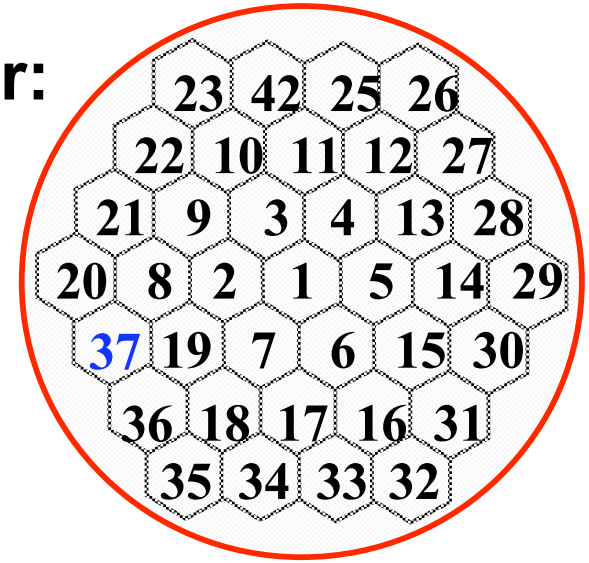

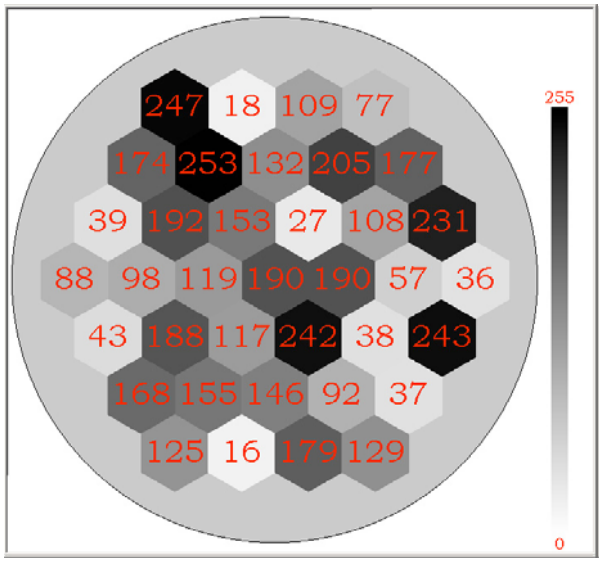

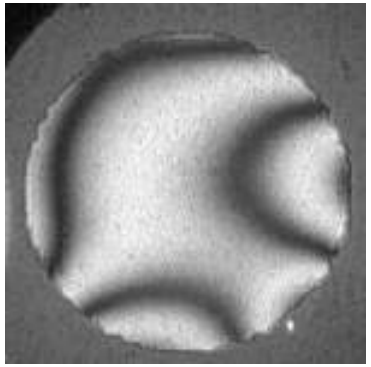

Initial State (All: 0V)

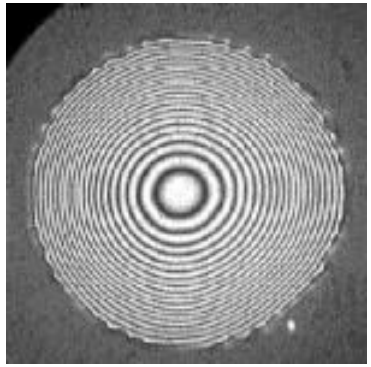

All: 125V

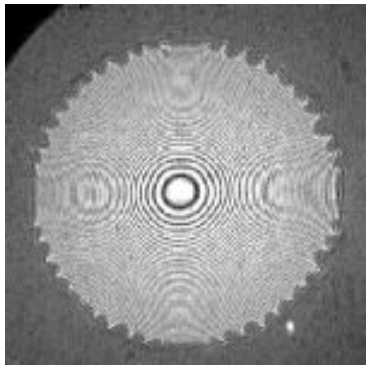

All: 255V (Max. Voltage)

Random Voltage

http://www.okotech.com/

2.4 Long-term stabilization of laser

1. Passive Stabilization (completed)

Stabilizing **environmental & mechanical** factors

↓

Reduction of**:**

- Optical damaging accidents

- Mechanical instability of optical components

2. Active Stabilization (in future)

- Automatic **boot-up**
- Automatic **adjustment** (AI-algorism)

3. Down-Sizing (in future)

2.4.1 Humidification for avoiding charge-up

Environmental test clean room

Constant Temperature & Humidity

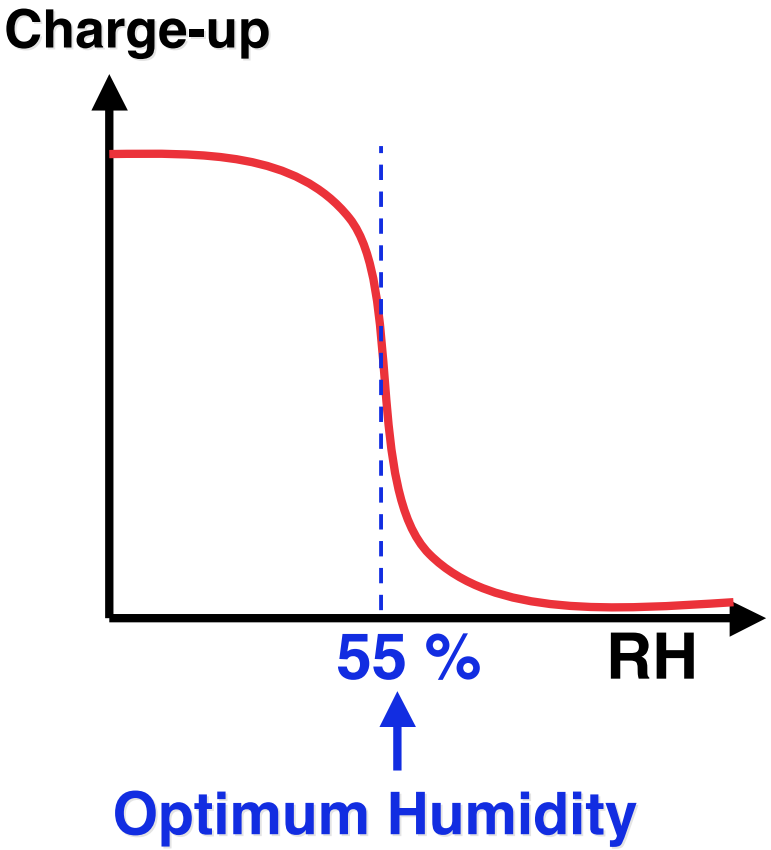

2.4.2 Long-term stabilization with water-cooling

3 ~ 5 % (rms) **After Passive control** → **@THG (263 nm)** *1.3 ~ 1.8 %* (rms)

Water-cooling for crystal
Suppress thermal lens effect:

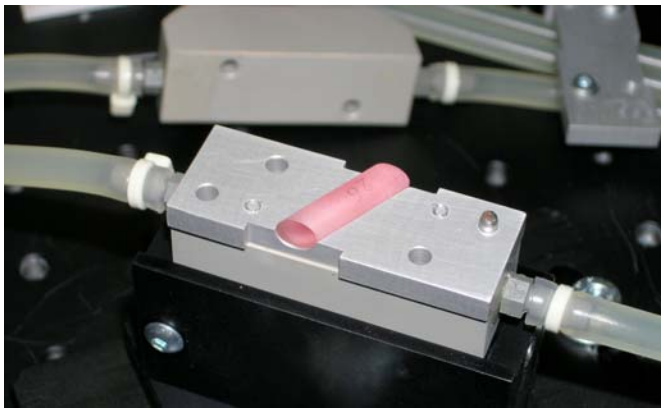

Water-cooling for base-plate
Fix deformation of laser-box:

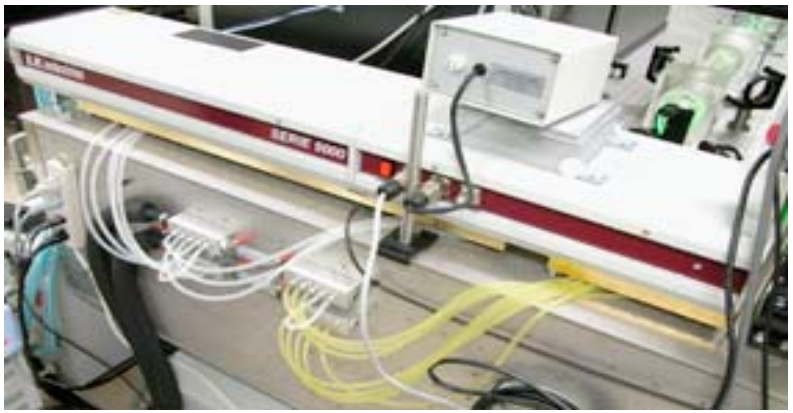

Water-cooling for Pockels Cell:
Suppress local heat-up:

2.4.3 Passive & Active stabilization of Oscillator

The most critical part of total laser stability

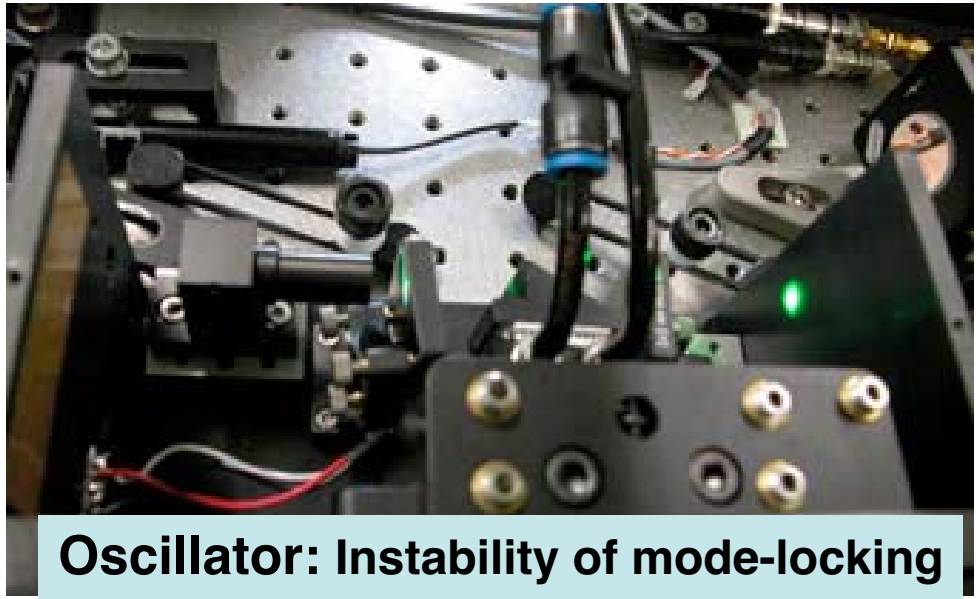

Oscillator: Instability of mode-locking

Replace conventional mirror holders with the thermal-deform-free ones

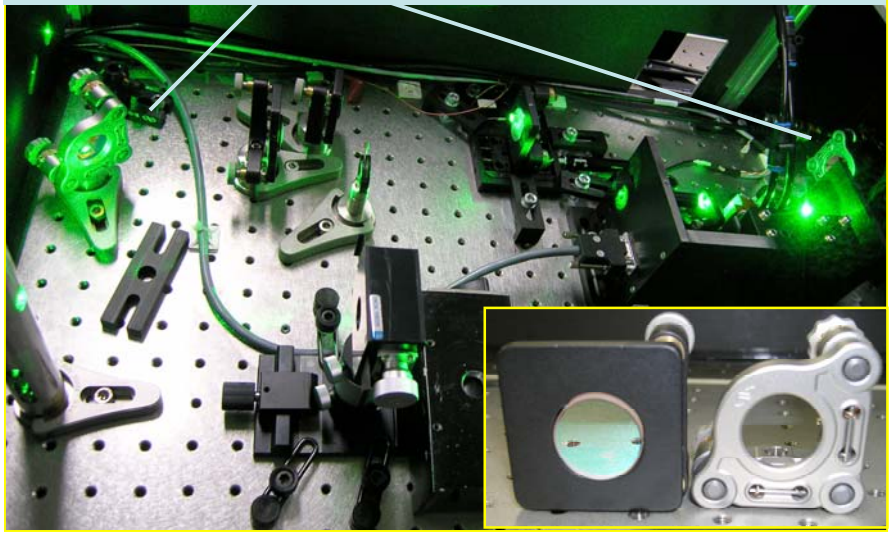

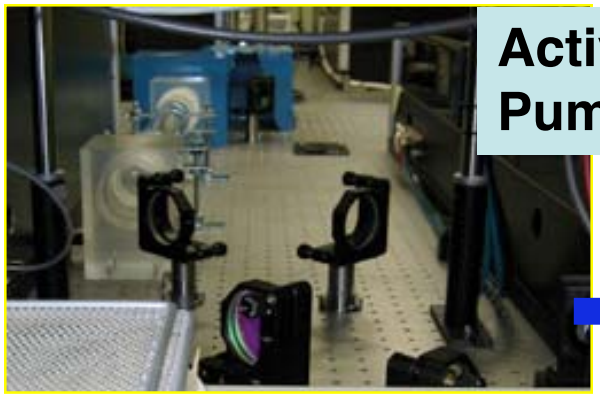

Active controlling optical pass of Pumping light source

3. Tracking Code & Cavity

3.1 Tracking Code

3.2 Pillbox cavity

3.3 Results of Emittance Measurement

3.4 Effects of oblique incidence of a laser

3.5 Etching-processed RF-gun cavity

& High Field Test

3.6 Second Booster Cavity

3.1 Tracking Code

Purpose for developing the 3D code

To investigate:

- **asymmetrical effects**, such as the spatial and temporal asymmetrical beam shapes
- **oblique incidence of a laser**
- asymmetrical RF fields

Characteristic of the code

- **Fully 3D**, including:
  - **space charge effect**
  - **image charge effect** of the cathode
- **A charged particle** is treated as **a macro particle**, which is a cluster of electrons
- **Electromagnetic fields** are calculated by the code **MAFIA**

Difficulty of the code

Many particles for precise calculation

→ much elapsed time

Scheme of the code

A) Force calculation between macro particles

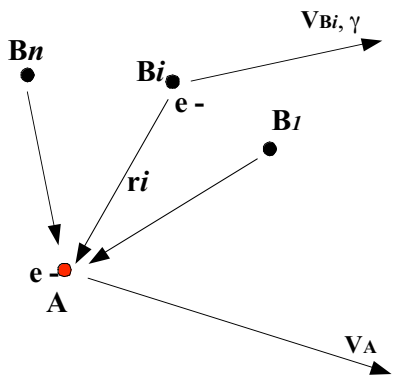

$$\mathbf{E}_A = \frac{1}{4\pi\varepsilon_0}\sum_{i=1}^{n}\frac{-e\mathbf{r}_i}{\gamma_i^2\left[|\mathbf{r}_i|^2 - \frac{|\mathbf{v}_{Bi}\times\mathbf{r}_i|^2}{c^2}\right]^{3/2}}$$

$$\mathbf{B}_A = -\frac{e}{4\pi\varepsilon_0 c^2}\sum_{i=1}^{n}\frac{\mathbf{v}_{Bi}\times\mathbf{r}_i}{\gamma_i^2\left[|\mathbf{r}_i|^2 - \frac{|\mathbf{v}_{Bi}\times\mathbf{r}_i|^2}{c^2}\right]^{3/2}}$$

$$\frac{d\mathbf{v}}{dt} = -\frac{e}{\gamma m_0}\left(\mathbf{v}\times\mathbf{B} + \mathbf{E} - \frac{(\mathbf{v}\cdot\mathbf{E})}{c^2}\mathbf{v}\right)$$

A: tracking particle

B*i*,(*i*=1,n): source particles for space charge

$$\mathbf{F}_A = -e(\mathbf{E}_A + \mathbf{v}_A\times\mathbf{B}_A) \rightarrow -e(\mathbf{v}\times\mathbf{B}+\mathbf{E}) = \frac{d\mathbf{P}}{dt} = m_0\frac{d(\gamma\mathbf{v})}{dt}$$

Runge-Kutta method

B) Definition of RF phase

$$E_{cavity} = E_{\max}\cos(\omega t - \phi)$$

C) Definition of emittance

$$\varepsilon_x = \gamma\beta\sqrt{<x^2><x'^2> - <x\cdot x'>^2}$$

3.2 Single-cell Test Cavity (First beam in 1999)

Low Q Cavity (Q ~2800, S-band)

$1/Q = 1/Q_0 + 1/Q_{ext}$

Shorter RF Pulse → Higher Field Gradient

Pure Water Rinsing → Dark Current Reduction

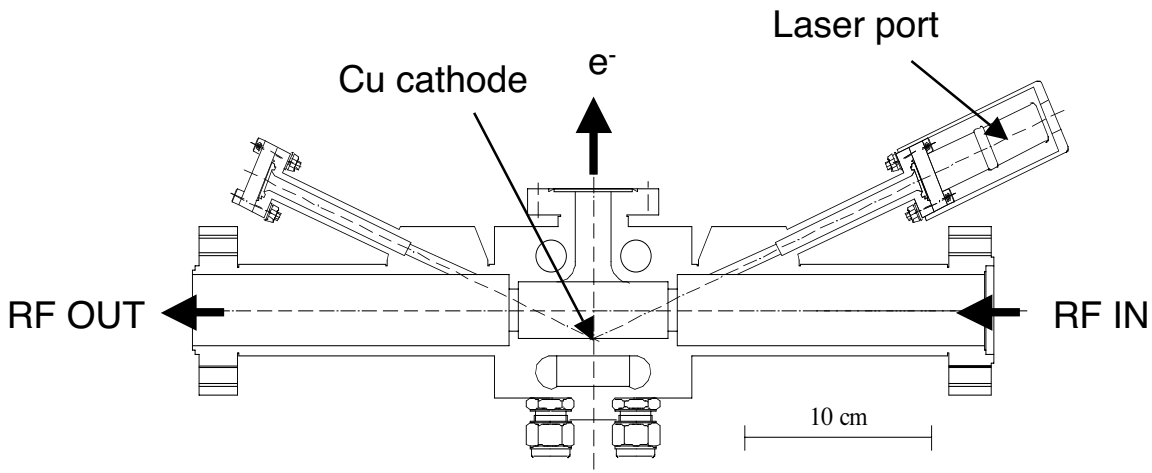

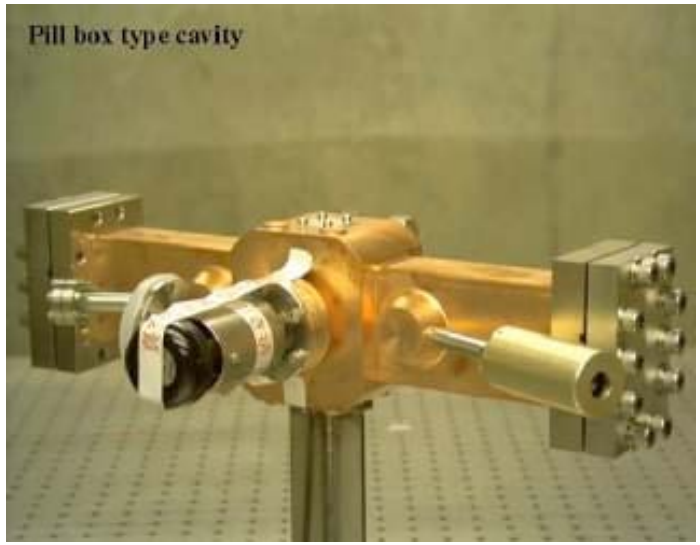

3.3 Results of Beam Emittance Measurement

(3.1-MeV E-Beam; direct after Gun; Double-Slit)

6.0 π mm mrad

May 2001

Laser System Improvement

2.3 π mm mrad

After Dec. 2001

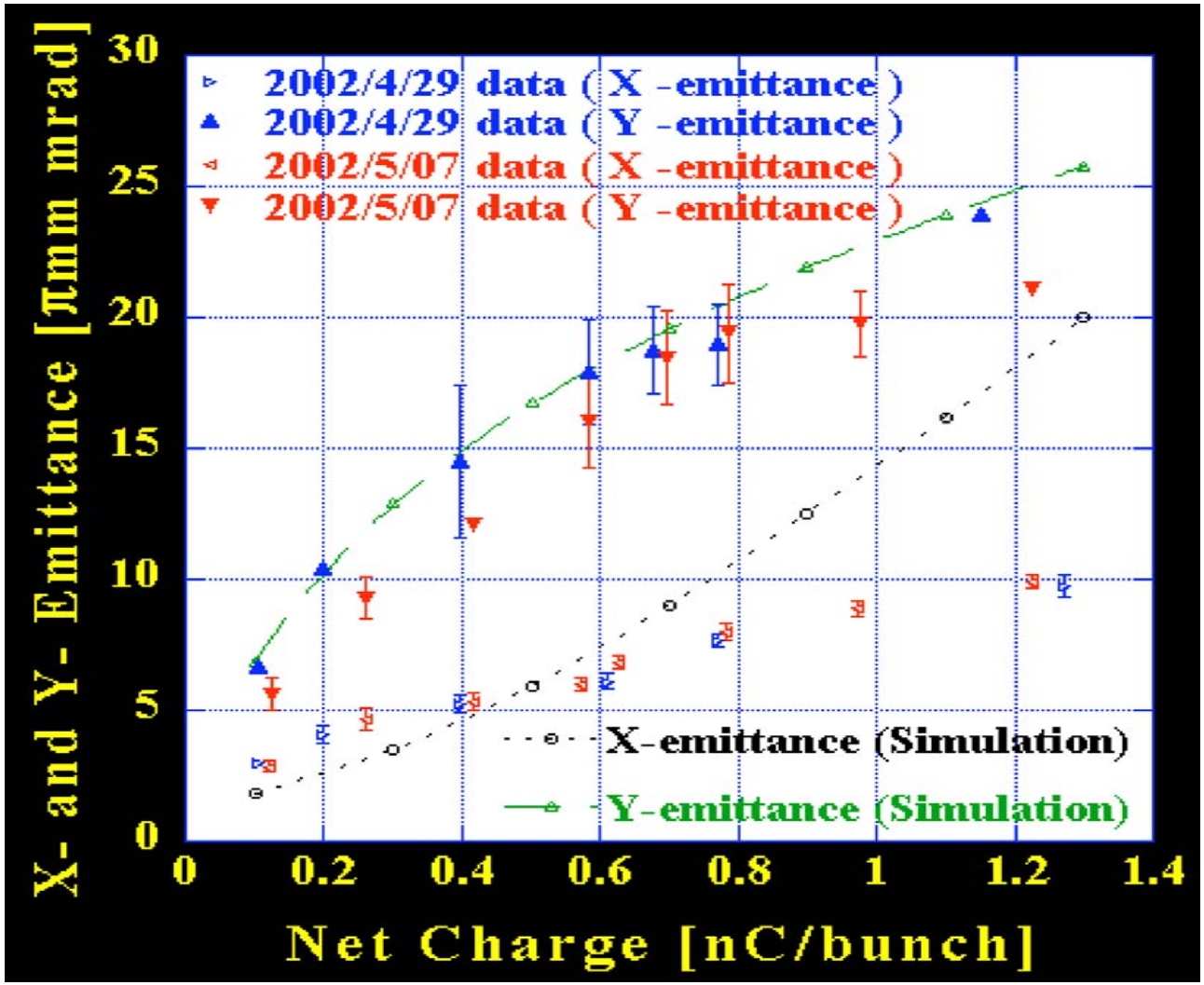

3.4 Effects of oblique incidence of a laser to the cathode

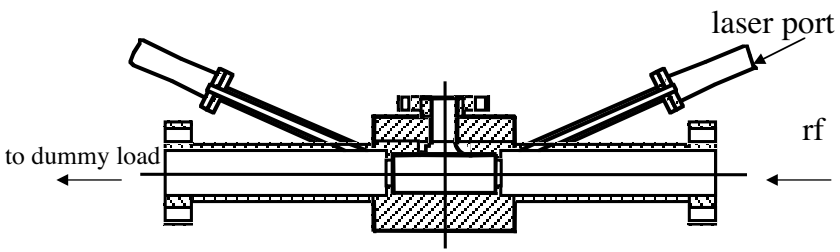

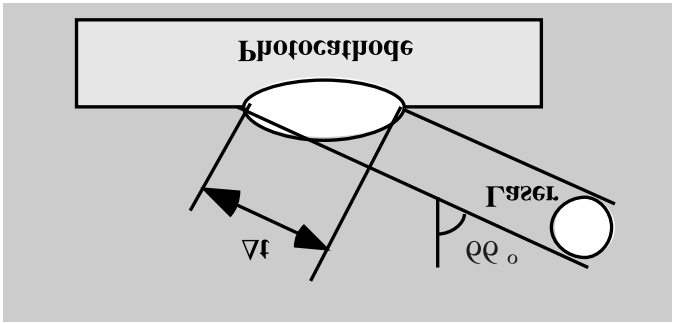

Time delay & elliptical laser shape

Parameters (for both experiment & our simulation code)

- Maximum field on the cathode: **135 MV/m**
- Initial RF phase : **85 degree**
- First solenoid coil : **1560 Gauss**
- Second solenoid coil : **780 Gauss**
- Laser incident angle : **66 degrees**
- Laser spot distribution: **Gaussian like figure**
- Laser spot radius : **0.3 mm (1s)**
- Laser temporal length: **5 ps (FWHM)**

$\varepsilon x < \varepsilon y$

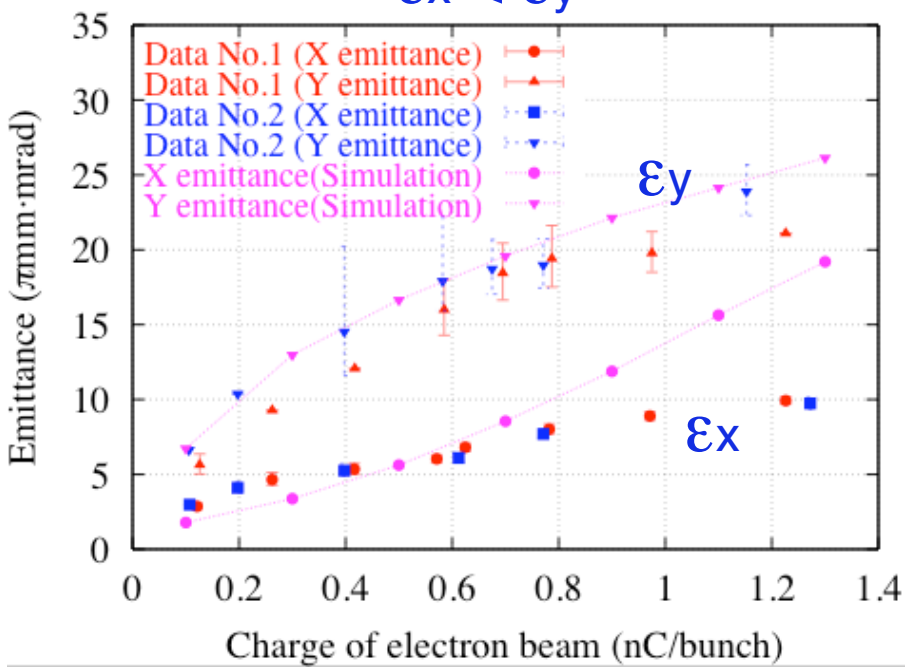

Lowest x-emittance value of 2.3 πmm•mrad was measured

3.5.1 Etching Process of RF-gun cavity

Chemical Etching ⇨ **Cleaning cathode surface**
No contamination
Least surface roughness

For high-field acceleration & high QE

Etching process

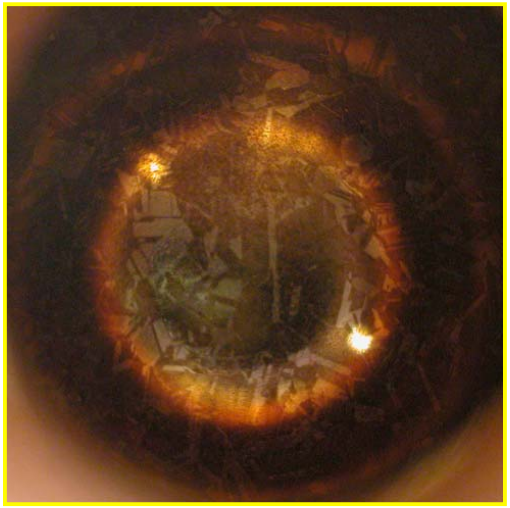

Cathode surface of RF gun after etching process

3.5.2 High Power Test for Etching-processed RF-gun cavity

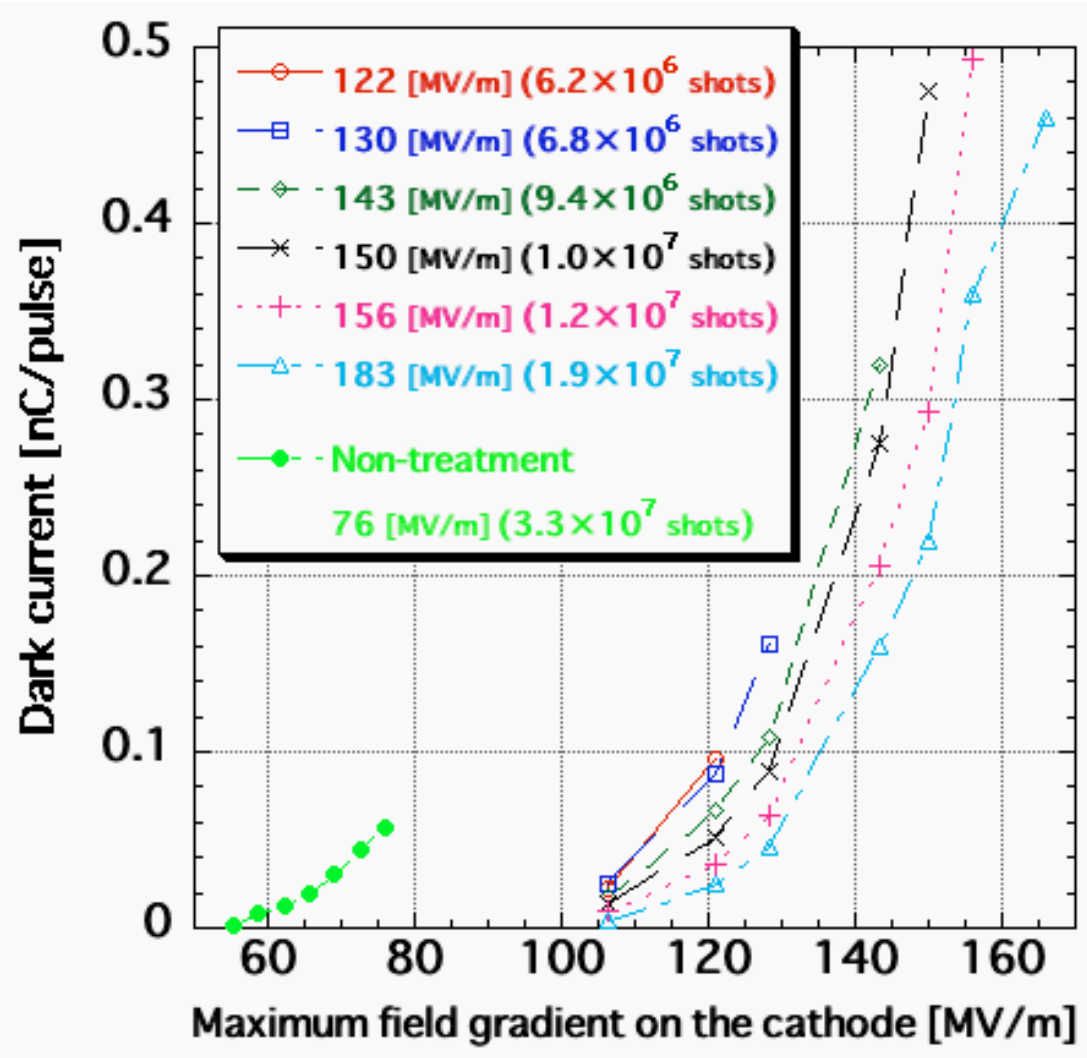

QE: **1 x 10^{-2} %**

Max. Cathode surface field:
190 MV/m

Max. surface field:
210 MV/m

3.6 Second Booster Cavity (in progress)

- Emittance reduction in higher charge region

Under design, to be fabricated in 2005

Tentative simulation
(PARMELA)

First cell: 135 MV/m
Second cell: 100 MV/m
6 MeV
1.4 nC/bunch
2.4 π mm mrad

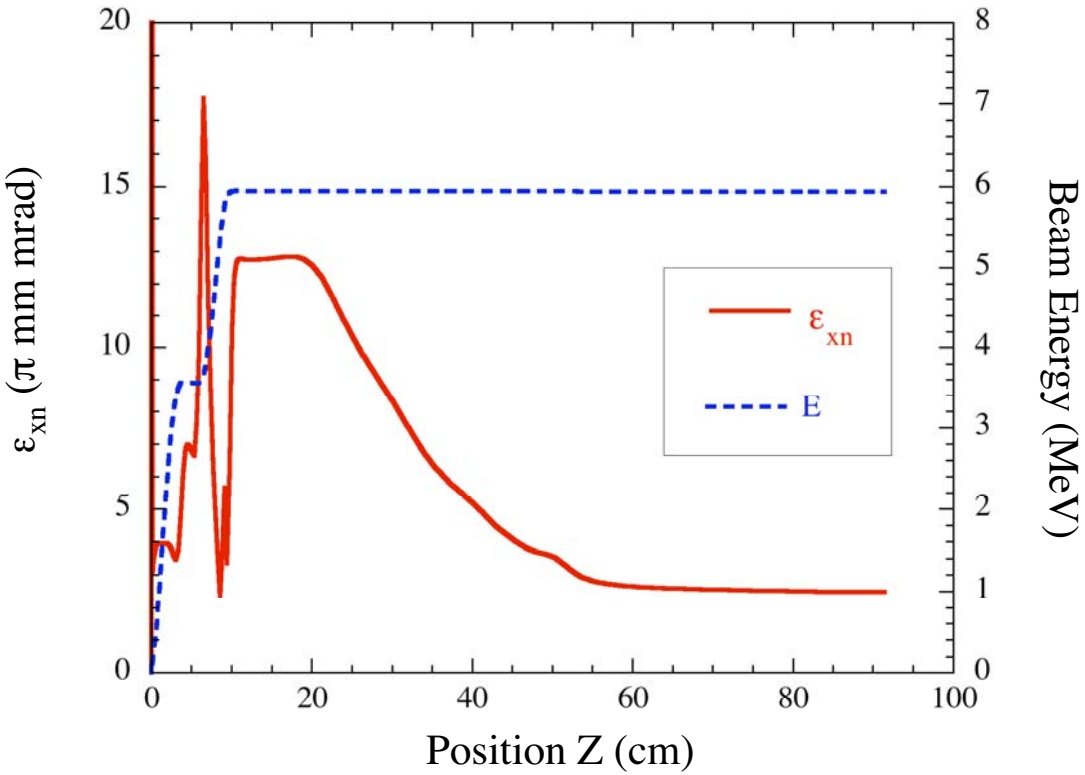

4. New Cathode Development

Collaboration with Hamamatsu Photonics Co.

- 4.1 Advantages of cartridge-type cathode
- 4.2 RF cavity & cathode loading system
- 4.3 Beam Test
- 4.4 Transparent-type structure
- 4.5 High QE photocathode
- 4.6 Diamond photocathode
- 4.7 New development

4.1 Advantages of Cartridge-type Cathode

- No need of cathode deposition chamber
  - no technical difficulties related to coating for users
  - quick exchange of a photocathode
  - stable QE value
  - low cost
- Easy to apply another kinds of photocathodes
- Transparent-type can be fabricated using photomultiplier technologies
- A cartridge holder can accommodate many cartridges without QE degradation.

Cartridge-type Cathode

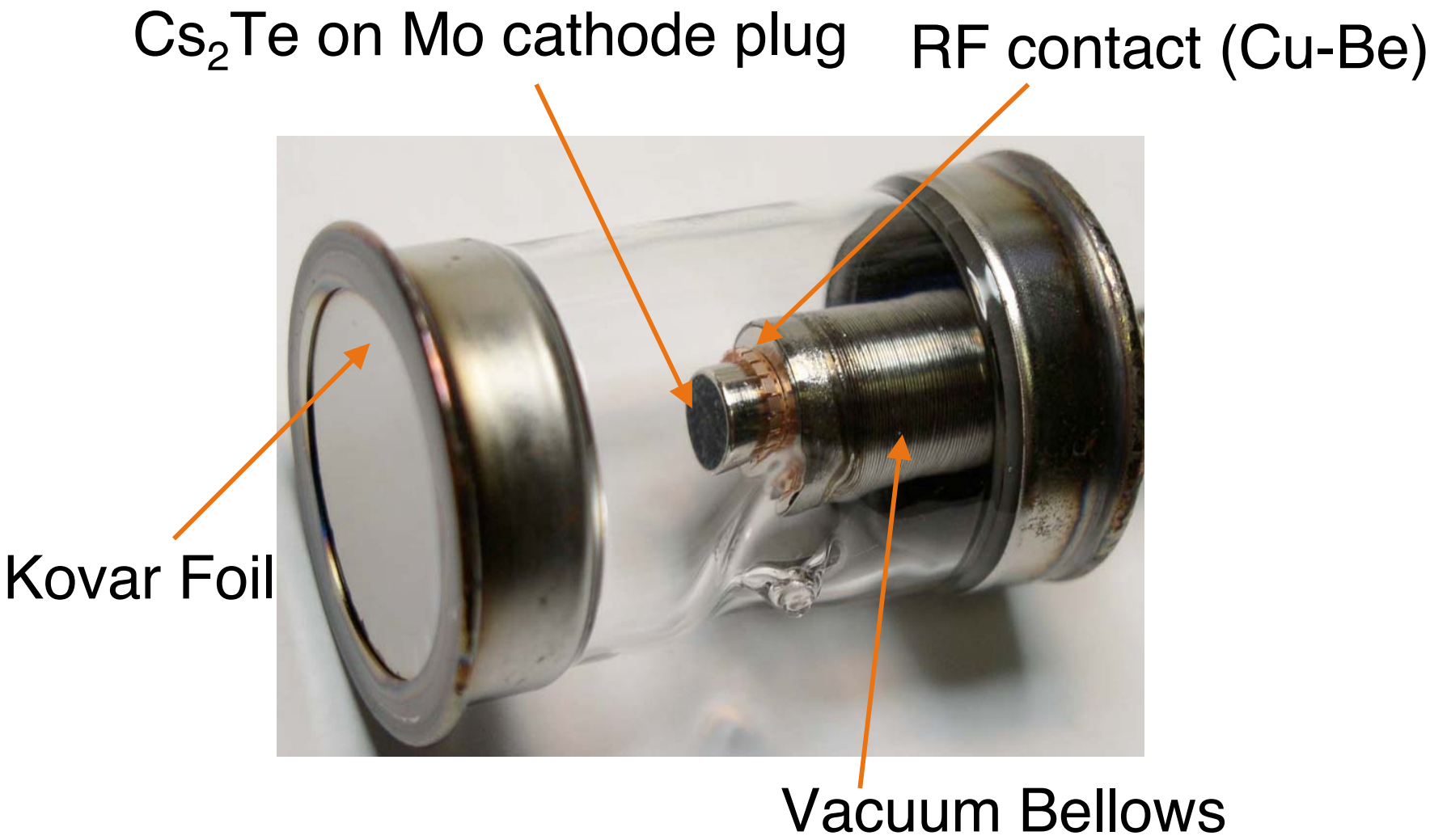

4.2 RF cavity & cathode loading system

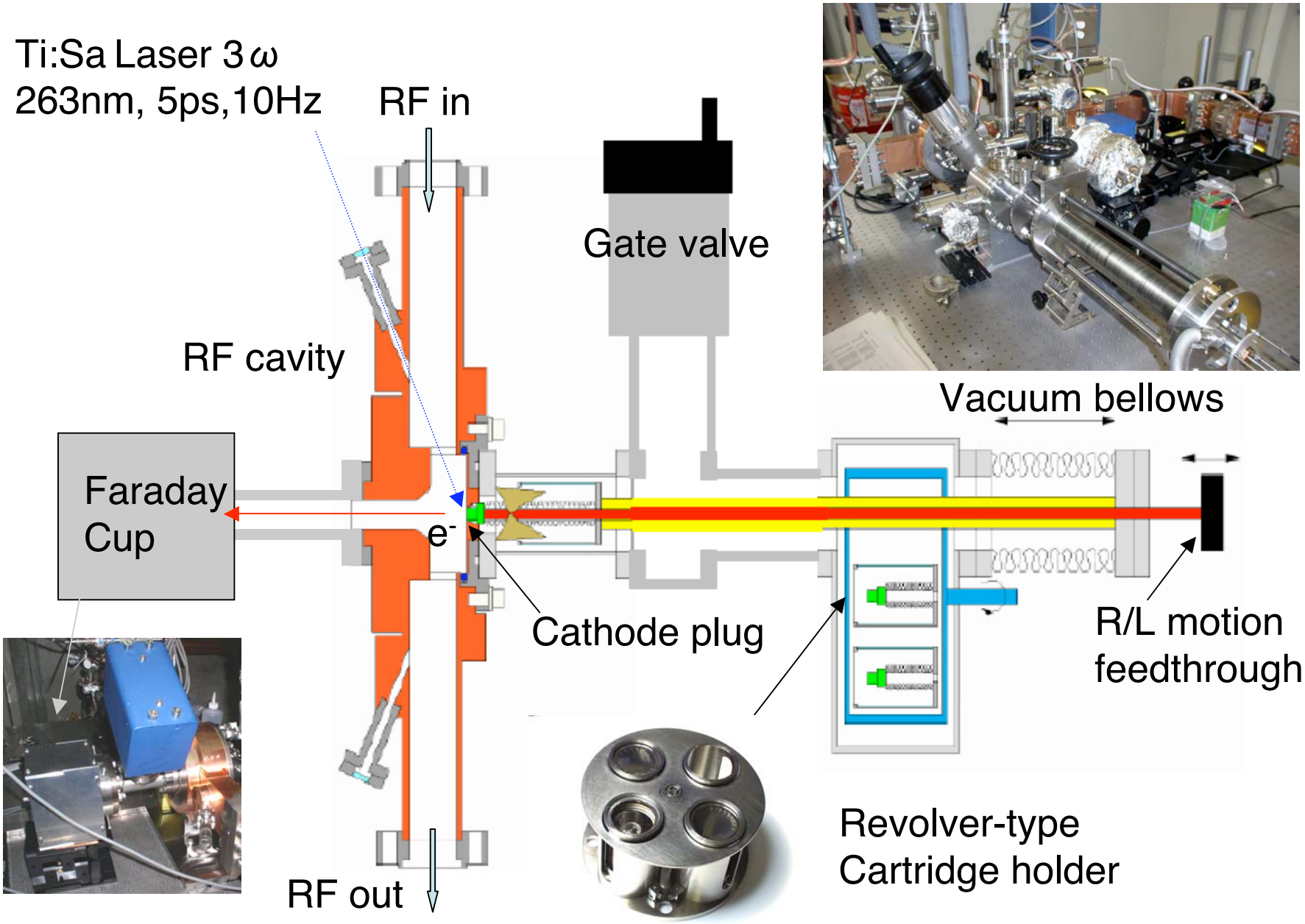

4.3 Beam Test

Temporal behavior of the QE during beam test

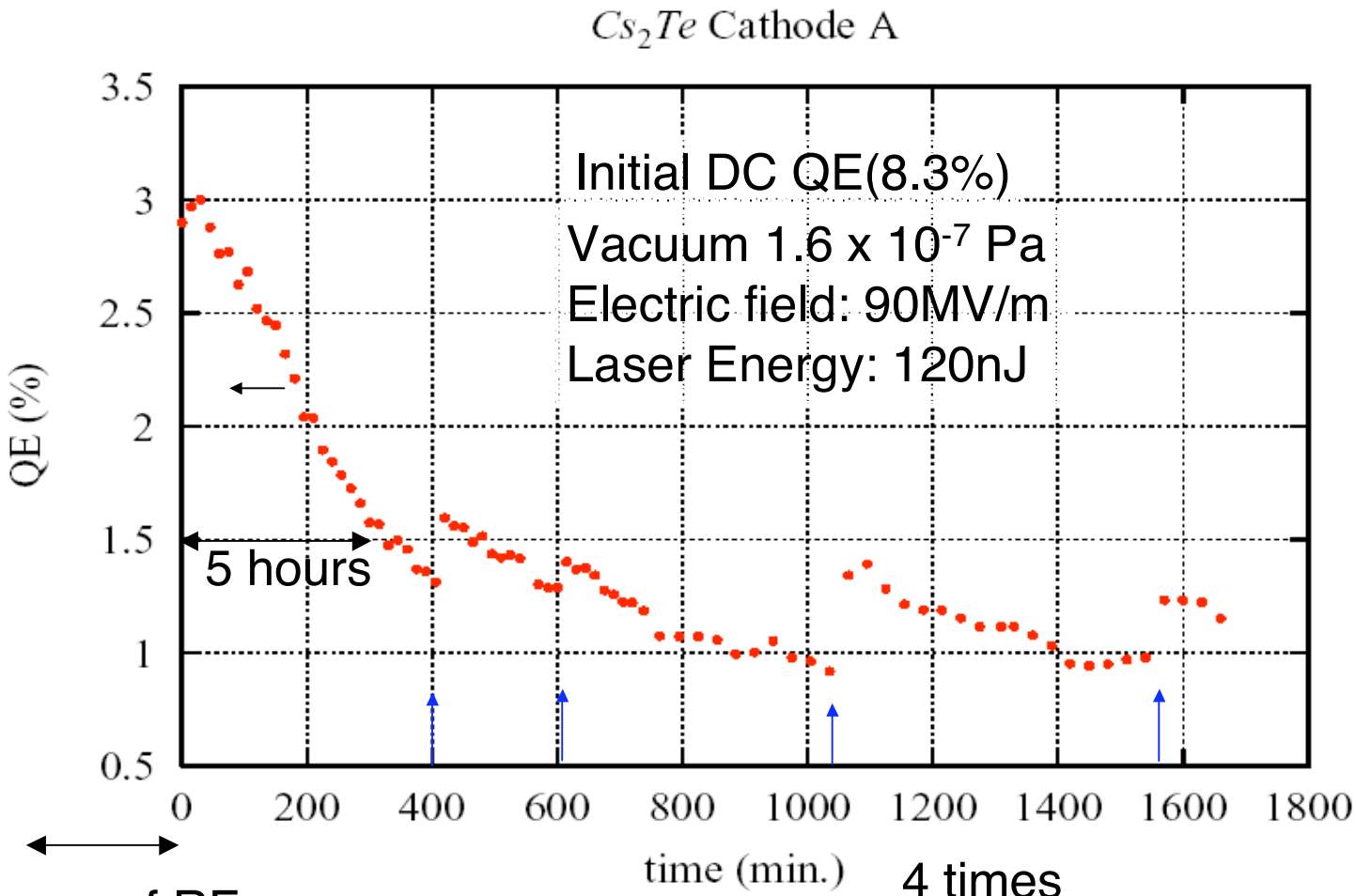

2 hours of RF processing

4 times Discharge

Why QE degrades rapidly?

- The degradation may be attributed to oxidization of the cathode surface.
- Outgassing during the RF processing may accelerate it.

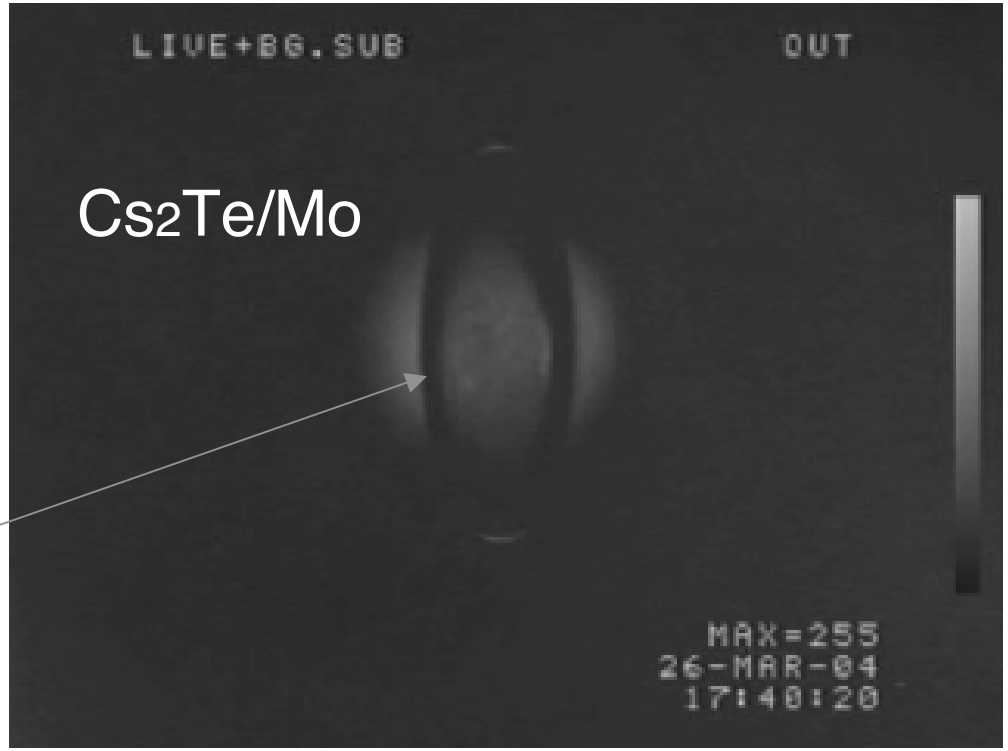

Cathode-plug

4.4 Transparent-type structure

- Complete perpendicular laser injection
- No reflecting mirror after the gun in vacuum
- Possibility of laser transport using glass fiber

First Trial: Sapphire substrate

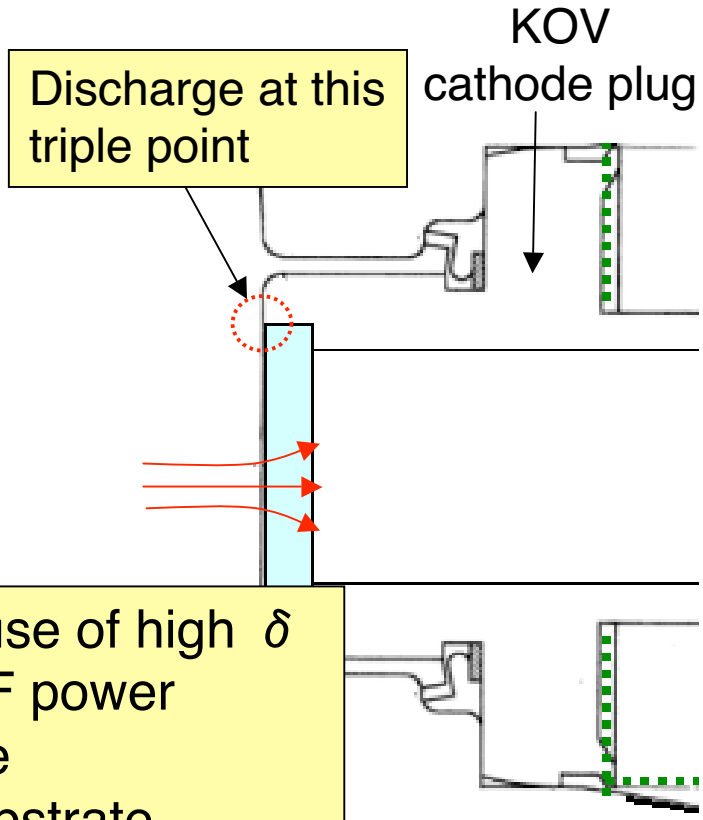

Sapphire substrate is easy to charge up because of high δ
---> Damage to photocathode, Reflection of RF power
Microwave is transparent to sapphire substrate
---> Electric field is not perpendicular to the substrate.

4.5 High QE Photocathode

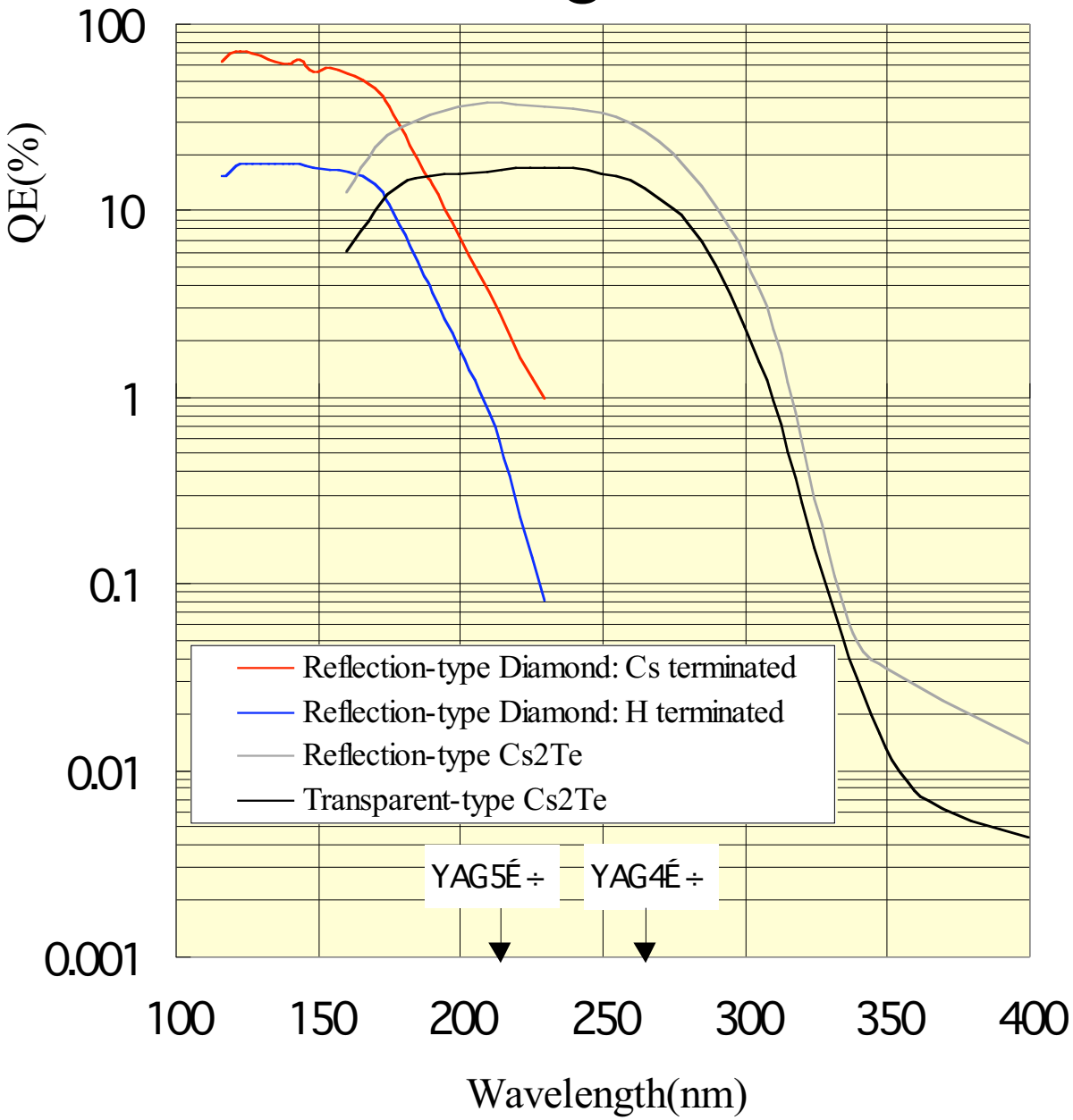

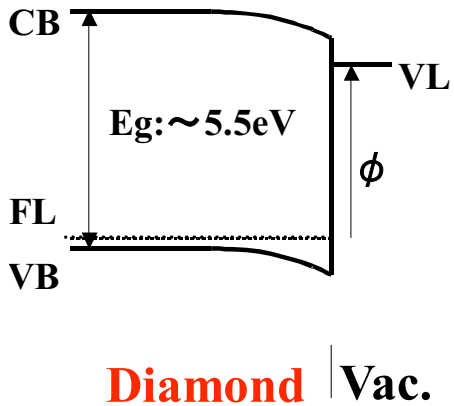

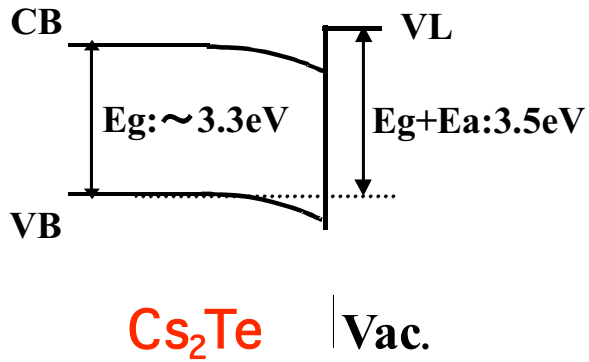

4.6 Diamond Photocathode

Characteristics of Diamond Photocathode

- Highest QE among all photocathodes (70%@125nm)
- Wide band-gap semiconductor (Eg=5.5eV)
- NEA photocathode
- Surface is chemically stable

  (no need of UHV)

QE data of Diamond Cathode before and after Air Exposure

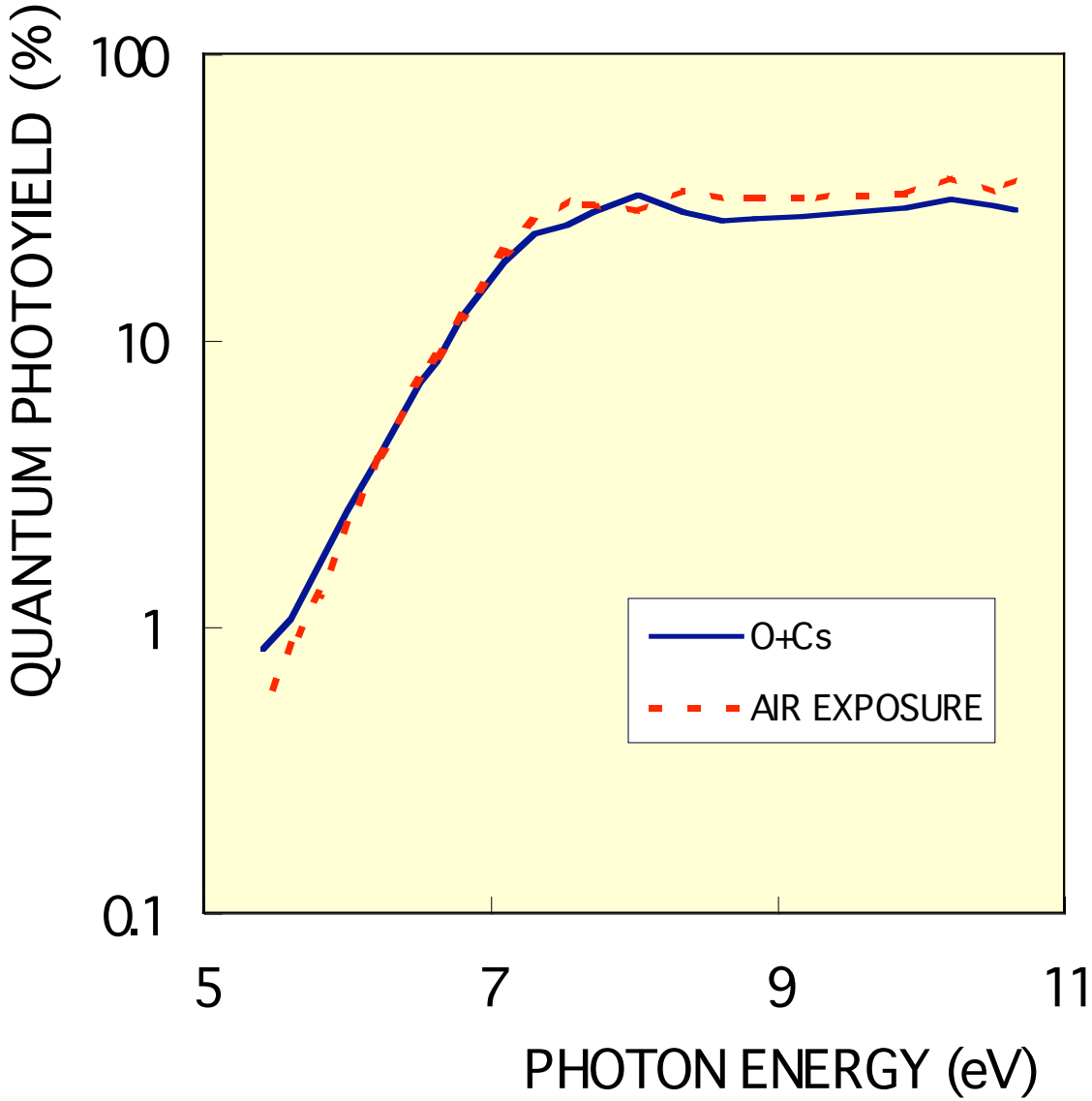

Diamond Photocathode

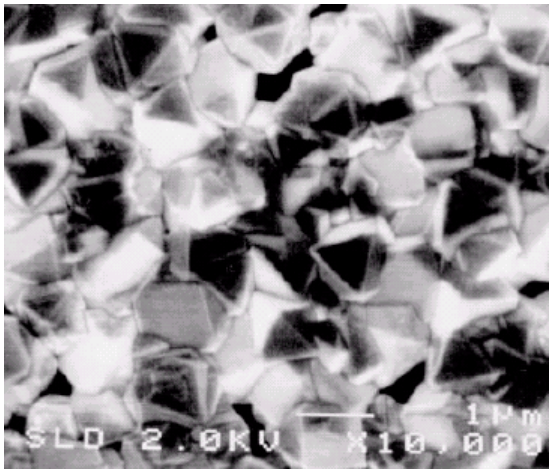

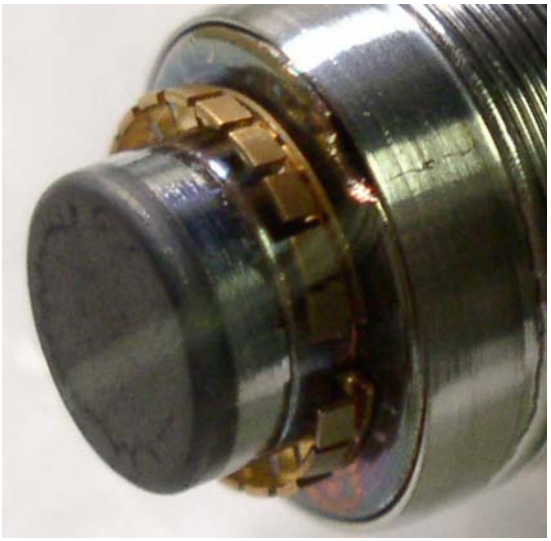

Dark Current of Diamond Photocathode

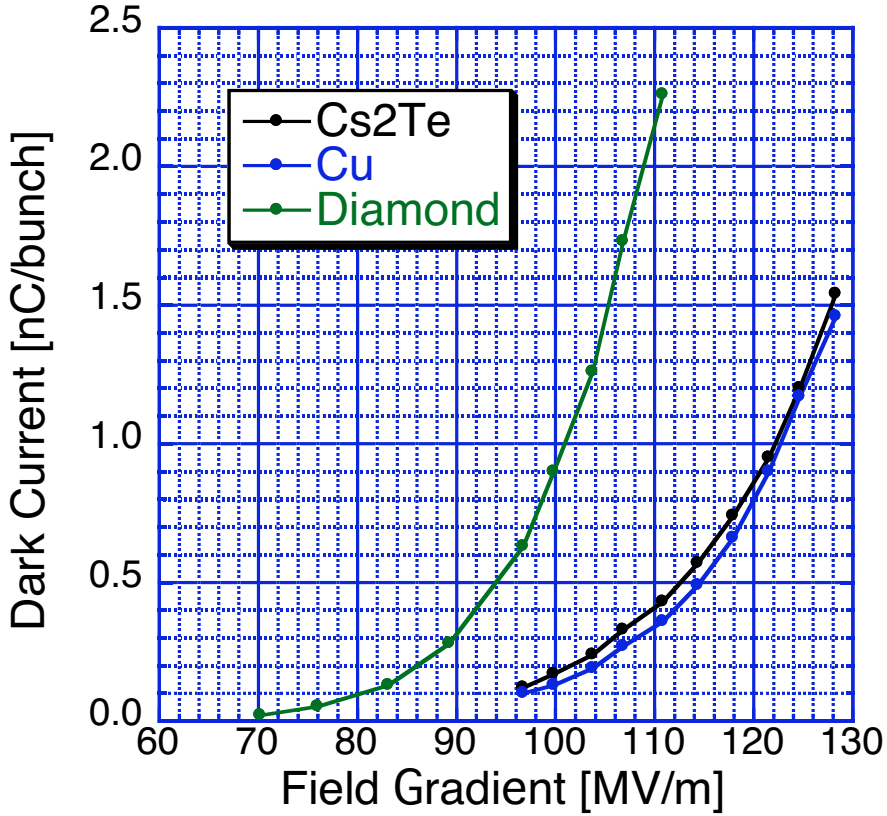

4.7 New Development

- Development of transparent-type Cs_2Te and Diamond photocathode
- New cartridge holder accommodates up to 12 cartridges

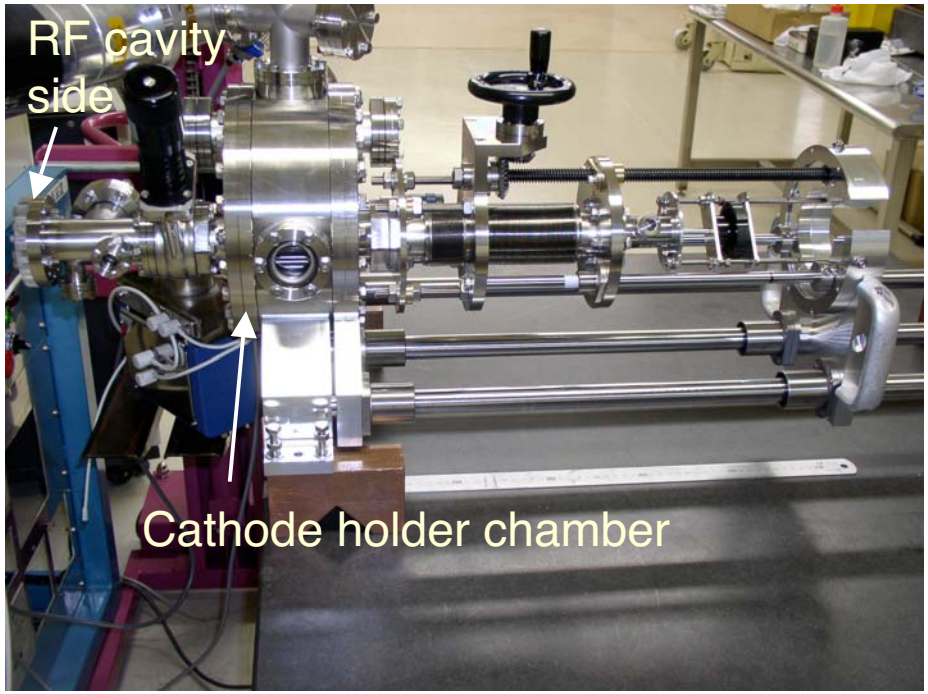

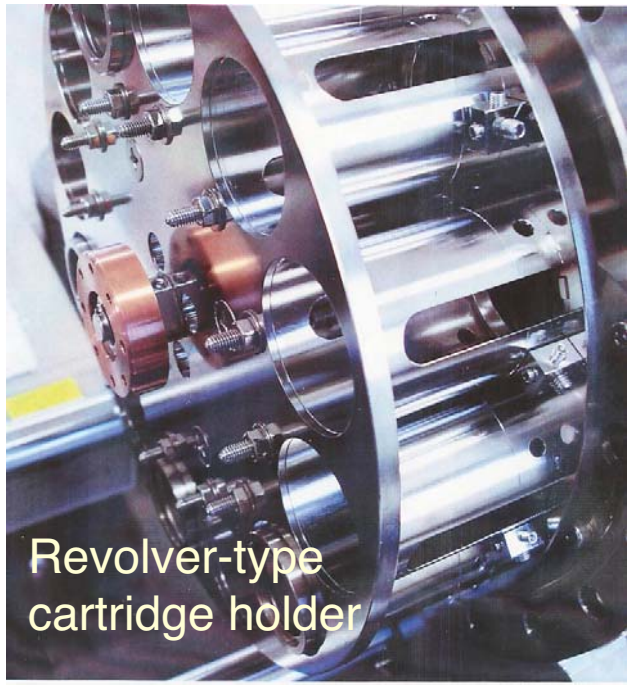

5. Emittance Measurements

- 5.1 Double slit @4MeV (Already Done)
  - High resolution for 3-4MeV region
- 5.2 Quad scan @30MeV (in Progress)
  - For linac energy region
- 5.3 Multislit@30MeV (Future)
  - One shot & linac energy region

5.1 Principle of Double Slits Measurement

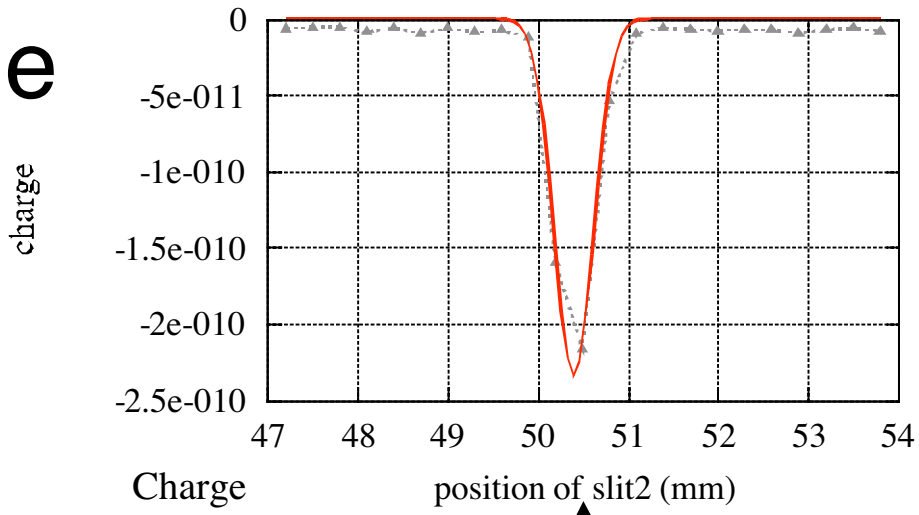

$$x' = \frac{d - x}{L}$$

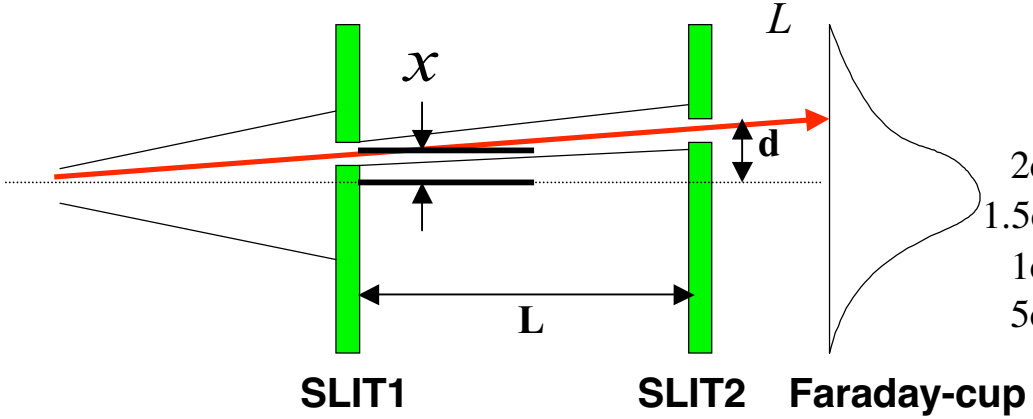

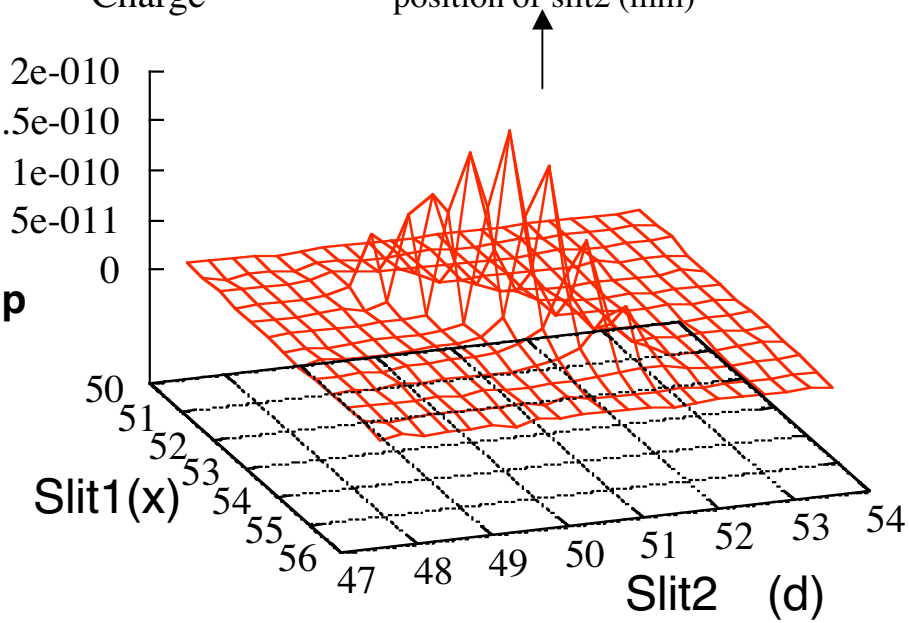

x	x'	Q
x_1	x'_1	Q_1
.	.	.
.	.	.
.	.	.
.	.	.
.	.	.
.	.	.
.	.	.
.	.	.
x_n	x'_n	Q_n

$$< x^2 >= \frac{\sum_i x_i^2 Q_i}{\sum_i Q_i}$$

$$< x'^2 >= \frac{\sum_i x_i'^2 Q_i}{\sum_i Q_i}$$

$$< x \cdot x' >= \frac{\sum_i x \cdot x' Q_i}{\sum_i Q_i}$$

Norm. RMS Emittance

$$\varepsilon =< \gamma >< \beta > \sqrt{< x^2 >< x'^2 > - < x \cdot x' >}$$

Outline of the Double Slit Emittance Measurements

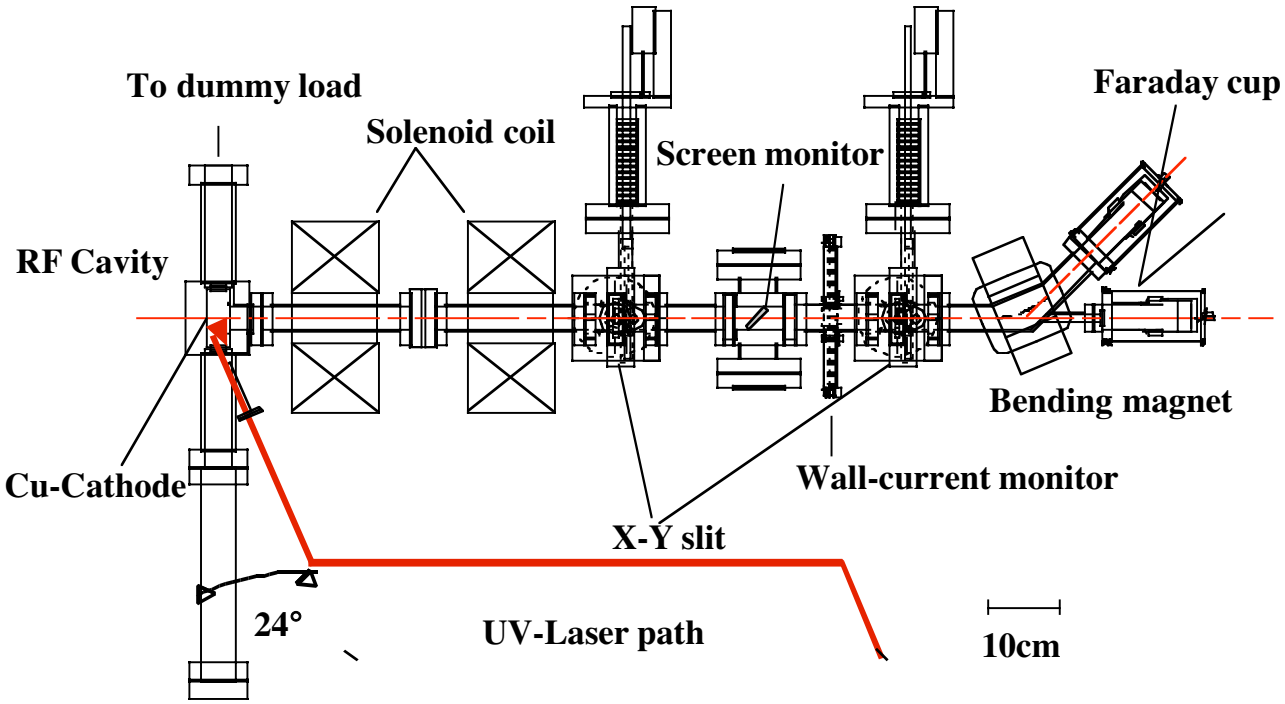

Copper Slit @thickness of 8 mm

Slit Width @0.3 mm & Two Slits Distance @ 460 mm

---> Resolution of RMS Norm. Emittance @ 0.42 πmmmrad

5.2 Quad Scan Measurement

To find the Lowest Emittance Conditions

↓

Need to evaluate the Beam Emittance quickly

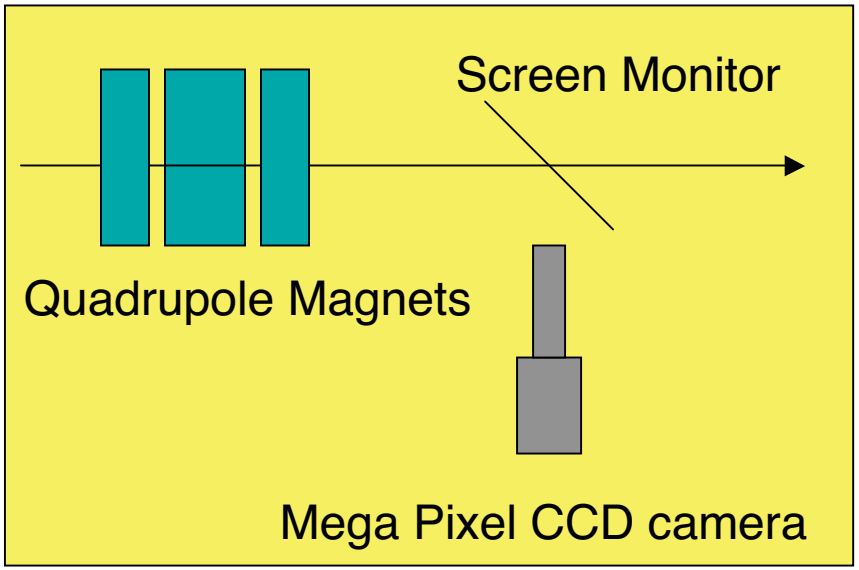

Automatic Emittance Measurement using Labview (in progress)

1. Scanning Q-magnet
2. Image capture
3. Measure Beam size

Repeat

Manual Test Measurement

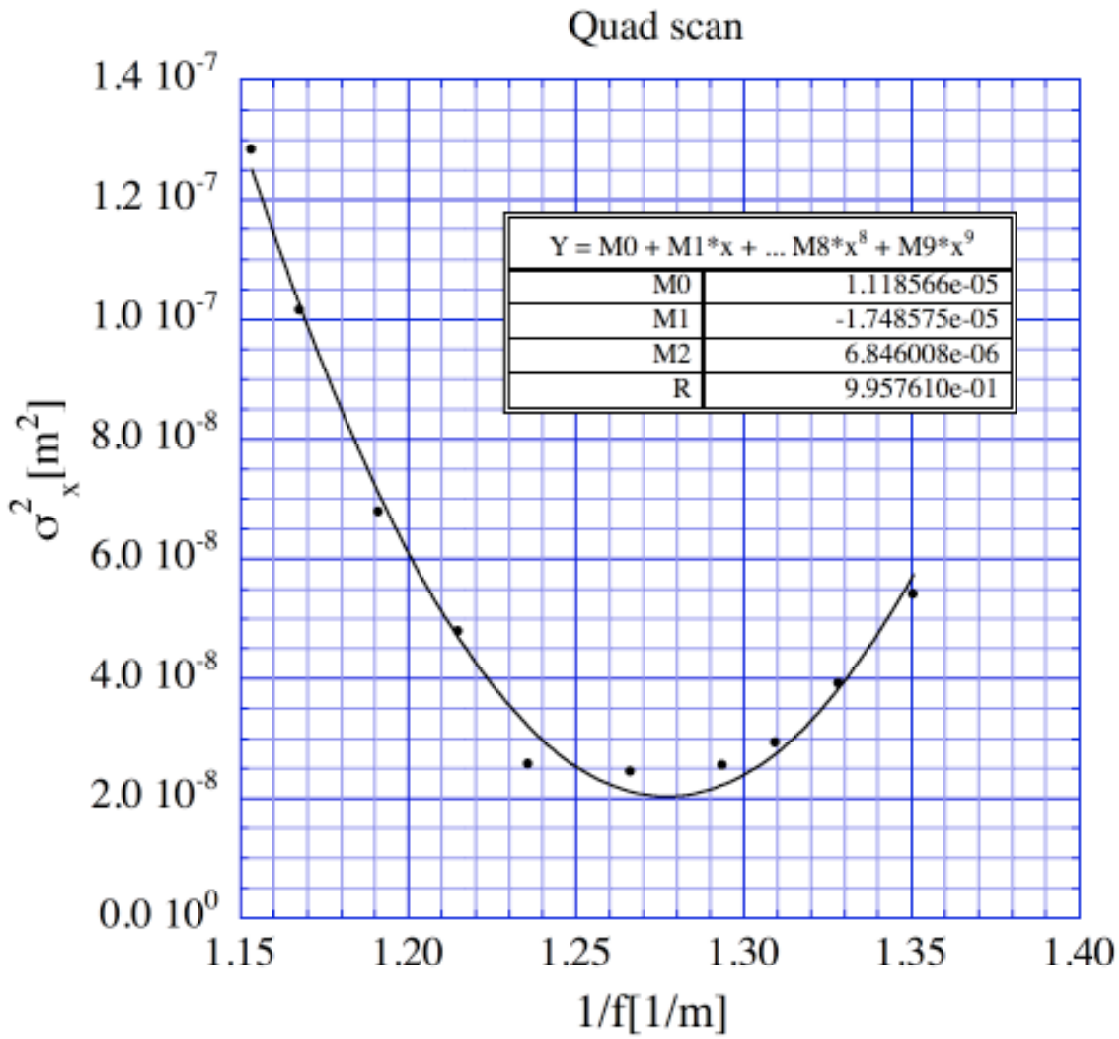

f: focal length of triplet

σ_x: rms beam size

Emittance: 10.9 πmmmrad

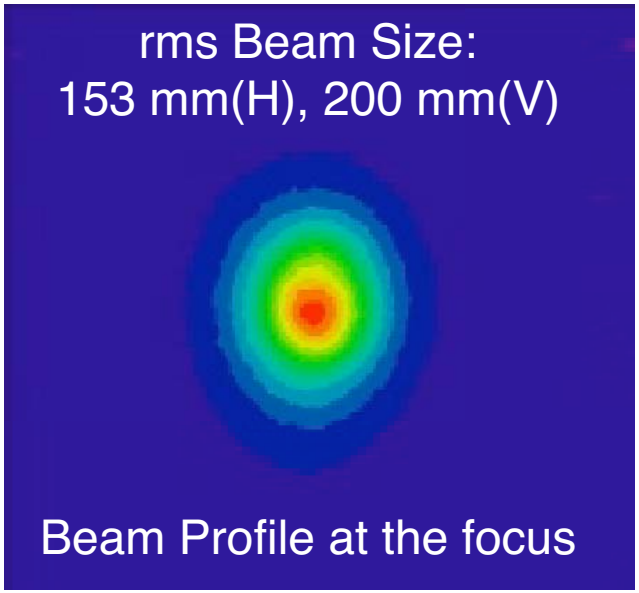

5.3 Multi Slits Emittance Measurement (in Progress)

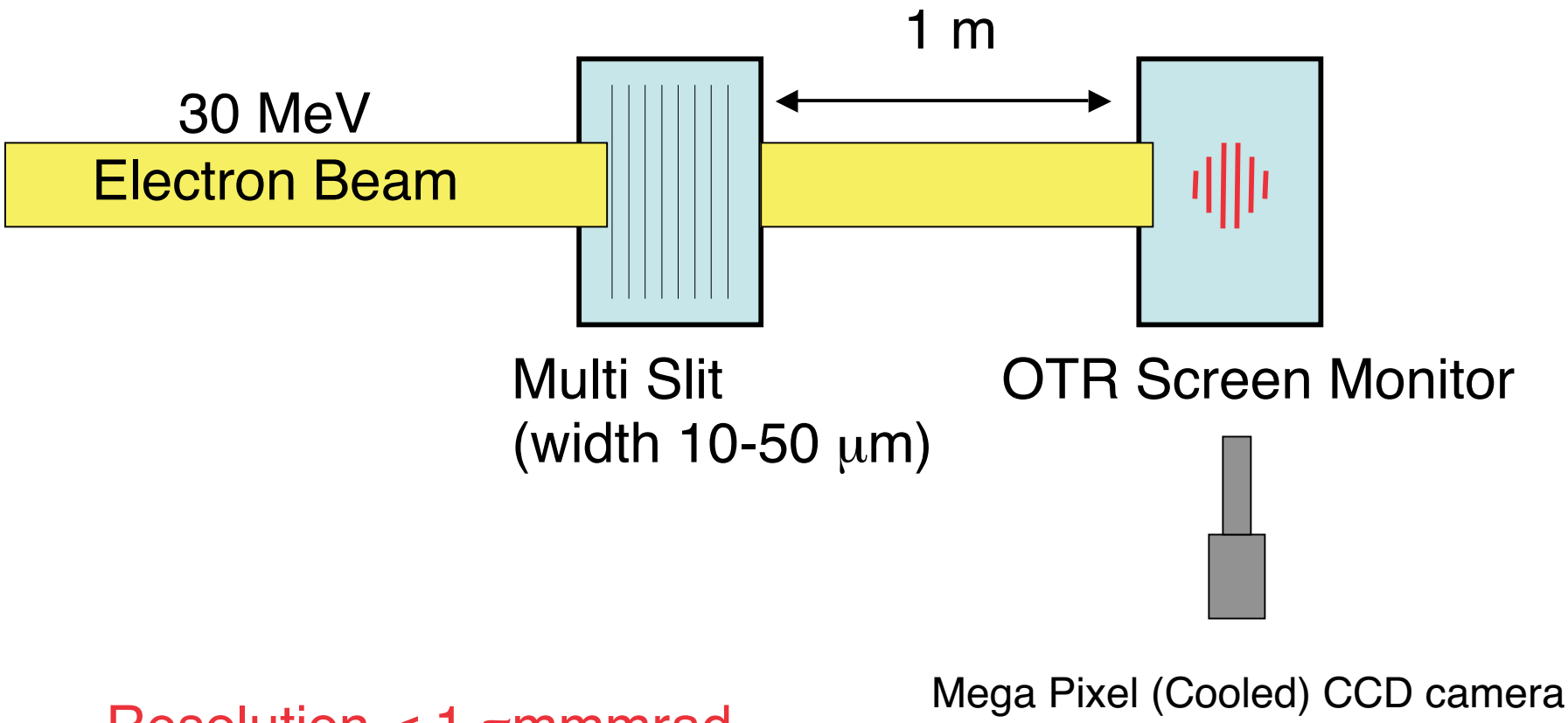

Resolution < 1 πmmmrad

One Shot Measurement

Summary

- Our purpose is generating lowest emittance electron beam.
- Low Emittance Beam can be generated and evaluated with
  - Well-shaped 3D-laser profile,
  - High Gradient Field,
  - High Resolution Emittance Monitor
- Cartridge-type Cathode may be easy to operate for future medical or industrial users as well as small laboratories.
- Transparent cathode might have a lot of possibilities, but currently have discharge problems.